15

MARYLAND

COLLEGE PARK CAMPUS

The Problem of Plate Modeling
Theoretical and Computational Results

by

I. Babuška

and

L. Li

Technical Note BN-1116

December 1990

INSTITUTE FOR PHYSICAL SCIENCE
AND TECHNOLOGY

Encl (1)

SECURITY CLASSIFICATION OF THIS PAGE (When Data Entered)

REPORT DOCUMENTATION PAGE

READ INSTRUCTIONS BEFORE COMPLETING FORM

1. REPORT NUMBER: Technical Note BN-1116	2. GOVT ACCESSION NO.
3. RECIPIENT'S CATALOG NUMBER	
4. TITLE (and Subtitle): The Problem of Plate Modeling - Theoretical and Computational Results	5. TYPE OF REPORT & PERIOD COVERED: Final life of the contract
6. PERFORMING ORG. REPORT NUMBER	
7. AUTHOR(s): I. Babuska [1] - L. Li	8. CONTRACT OR GRANT NUMBER(s): [1]ONR/N-00014-90-J-1030 NSF/CCR-88-20279
9. PERFORMING ORGANIZATION NAME AND ADDRESS: Institute for Physical Science and Technology, University of Maryland, College Park, MD 20742	10. PROGRAM ELEMENT, PROJECT, TASK AREA & WORK UNIT NUMBERS
11. CONTROLLING OFFICE NAME AND ADDRESS: Department of the Navy, Office of Naval Research, Arlington, VA 22217	12. REPORT DATE: December 1990
	13. NUMBER OF PAGES: 60
14. MONITORING AGENCY NAME & ADDRESS (if different from Controlling Office)	15. SECURITY CLASS. (of this report)
	15a. DECLASSIFICATION/DOWNGRADING SCHEDULE

16. DISTRIBUTION STATEMENT (of this Report)

Approved for public release: distribution unlimited

17. DISTRIBUTION STATEMENT (of the abstract entered in Block 20, if different from Report)

18. SUPPLEMENTARY NOTES

19. KEY WORDS (Continue on reverse side if necessary and identify by block number)

Plates, Kirchhoff model, Reissner-Mindlin model, plate paradox, corner signatures

20. ABSTRACT (

The paper analyzes in detail the problem of various plate models, properties of their solution and the question how well these models approximate the 3-dimensional formulation. The boundary layer and corner singularities of the solution are analyzed. A hierarchy of the models converging to the 3-dimensional solution is constructed. The detailed numerical computations show various basic aspects of plate modeling in a concrete setting.

DD FORM 1 JAN 73 1473 EDITION OF 1 NOV 65 IS OBSOLETE

S/N 0102-LF-014-6601

SECURITY CLASSIFICATION OF THIS PAGE (When Data Entered)

The problem of plate modeling

Theoretical and computational results

I. Babuška,* L. Li†

MD90-42-IBLL

TR90-42

---

* Institute for Physical Science and Technology, University of Maryland, College Park, Maryland, 20742

† Department of Mathematics, University of Maryland, College Park, Maryland, 20742, and Department of Mathematics, Fudon University, Shanghai 200020, People's Republic of China.

The first author was partially supported by Office of Naval Research grant N-00014-90-J-1030 and National Science Foundation grant CCR-88-20279.

Abstract.

The paper analyzes in detail the problem of various plate models, properties of their solution and the question how well these models approximate the 3-dimensional formulation. The boundary layer and corner singularities of the solution are analyzed. A hierarchy of the models converging to the 3-dimensional solution is constructed. The detailed numerical computations show various basic aspects of plate modeling in a concrete setting.

Key Words: Plates, Kirchhoff model, Reissner-Mindlin model, plate paradox, corner singularities

1. Introduction.

The plate and shells are basic elements in structural mechanics. Historically much attention has been given to the derivation of plate and shell models which lead to the different solution depending on the model used; see e.g. [1] for a survey. The derivation of a model is typically based on various mechanical considerations and principles. Only in 1959 in [2] was the first rigorous proof of the relation between the three-dimensional solution and the plate model given.

Many papers then had analyzed the plate theories via asymptotic analysis. See e.g., [3] and [4] and references there. Current development of numerical methods leads to the understanding of the plate and shell modeling as the application of the dimensional reduction principles to the three-dimensional problem. This then leads to a hierarchical modeling and to a convergent sequence of models. Adaptive approaches together with the a-posteriori analysis of the error of the model is a realistic goal to be

achieved.

The recent development of the h-p version of the finite element method allows to create a natural hierarchy of models based on the polynomial approximation through the thickness and the use of the variational approaches. Such approximation is in a certain sense optimal. See e.g. [5]. The h-p version also allows for assessing the *accuracy of the finite element solution* when compared with the exact solution of the plate model under consideration, as well as the error when compared with the three-dimensional solution.

In this paper we discuss the accuracy of various plate models when compared with the solution of the three-dimensional problem. Although the 3-dimensional solution is not exactly known, we can find it by numerical means. The error lies in a tolerance bracket which is adjusted to the aims of our analysis. Hence we can assume that the 3-dimensional solution is available. The accuracy control is based on the comparison of the solution for various meshes and degrees of elements. The computation was made by the program MSC/PROBE with h-p capabilities.

Typically we deal with a uniformly loaded square plate, $|x_i| < 0.5$, $i = 1,2$, with the plate thickness $d = \frac{1}{100}$. Because of symmetries, the problem is solved for the quarter only. The basic mesh in the quarter of the plate is defined by the lines $x_1 = \xi_i$, $x_2 = \xi_i$ with various meshes

1) 25 elements:
   $\xi_i = 0,\ 0.36,\ 0.492.\ 0.4994,\ 0.49988,\ 0.5$
2) 36 elements:
   $\xi_i = 0,\ 0.3,\ 0.36,\ 0.492,\ 0.4994,\ 0.49988,\ 0.5$
3) 81 elements:
   $\xi_i = 0.15,\ 0.25,\ 0.36,\ 0.43,\ 0.47,\ 0.492,\ 0.4994,\ 0.49988,\ 0.5$

and additional mesh refinement in the corner if the solution is singular. Also other plates shapes are considered in the paper. We assume homogeneous isotropic material with Poisson ratio $\nu = 0.3$.

In Section 2 we define the plate problem as a three-dimensional problem of elasticity and give basic preliminaries.

In Section 3 we define a hierarchical family of plate models.

Section 4 deals with the problem of the simply supported plate. In the first part, 4.1, we discuss the definition of the hard and soft support for a 3-dimensional formulation. We introduce various theorems showing that as $d \longrightarrow 0$, the difference between the two supports disappears when measured in the energy norm. A paradoxical behavior of the hard support shows that the difference between hard and soft support need not necessarily be constrained to the small neighborhood of the boundary. It depends on the structure of the boundary of the plate. In 4.1 we discuss the singular behavior of the three-dimensional solution in the neighborhood of the edges and vertices and the behavior of the moments and shear forces computed from it.

Section 4.2 presents detailed numerical results for the uniformly loaded square plate (in 3 dimensions) which serves in the next section as the exact solution. We concentrate on the difference of moments and shear forces for the soft and hard supports and descriptions of the boundary layer.

Section 4.3 describes the family of the dimensionally reduced problems and formulates various pertinent theorems. The well-known Reissner-Mindlin model appears as one member of this family. The theoretical behavior of the solution of these models in the neighborhood of the domain corners is presented.

Section 4.4 reports various numerical results. It shows the accuracy of the solution of various models when compared with 3-dimensional solutions for

the hard and soft support. The boundary layer and the character of the solution in the neighborhood of a vertex is addressed.

In Section 4.5, we address the problem of the L-shaped domain for the soft simple support. The main emphasis is given to the theoretical and numerical analysis of the solution's behavior in the neighborhood of the vertex with the concave angle. The main characteristic difference in the comparison with the case of square domain is shown . It is shown, among other things, that the different models have solutions with the different strengths of the singularity.

Section 4.6 analyzes the Kirchhoff model. It is shown here, for example, that the Kirchhoff model essentially approximates the hard support and the classical computation of the reaction is an attempt to get the value of the reaction for the soft support.

Section 4.7 summarizes the results presented in Section 4.

Section 5 discusses some other boundary conditions. In Section 5.1 the case of square clamped plates is analyzed. It is shown among others, that the Reissner-Mindlin model which captures well the boundary layer of the 3-dimensional solution for the simple support is completely missing a strong boundary layer for the clamped boundary condition.

Section 5.2 addresses then the square plate which is clamped on two opposite sides and free on two opposite sides. Attention is given to the behavior of the solutions of various models in the neighborhood of the vertices.

Section 6, the final one, makes additional remarks and some basic conclusions.

2. Basic notations and preliminaries.

Let $\omega \in \mathbb{R}^2$ be a polygonal domain with the boundary Γ and $\Omega = \{x = (x_1,x_2,x_3) \in \mathbb{R}^3 \mid (x_1,x_2) \in \omega, \ -\frac{d}{2} < x_3 < \frac{d}{2}\}$; Ω will be called the plate of thickness d. Further let

$$S = \{x \in \mathbb{R}^3 \mid (x_1,x_2) \in \Gamma, \ -\frac{d}{2} < x_2 < \frac{d}{2}\} \quad \text{and}$$

$$R_{\pm} = \{x \in \mathbb{R}^3 \mid (x_1,x_2) \in \omega, \ x_3 = \pm\frac{d}{2}\}$$

By the (exact) *solution* of the plate problem, we will understand the solution of the three-dimensional linear elasticity problem for an isotropic homogeneous material when the equal normal load is acting on $R_{\pm}$. More precisely denoting $T = (T_1,T_2,T_3)$ the traction vector, we assume $T_1 = T_2 = 0$ on $R_{\pm}$ and $T_3 = \frac{1}{2}q(x)$, $x \in \omega$ on $R_{\pm}$. On S various homogeneous boundary condition, which will be specified later will be considered. By $u = \{u_i\}$, $i = 1,2,3$, and $e = \{e_{ij}\}$, $i,j = 1,2,3$, $\sigma = \{\sigma_{ij}\}$, $i,j = 1,2,3$ we denote the displacement vector, the strain tensor and the stress tensor.

Let $A = \{a_{ij}\}$, $i,j = 1,\ldots,6$ be the Hooke's law matrix (compliance matrix) relating the strain and stress

$$(2.1) \qquad \begin{bmatrix} \sigma_{11} \\ \sigma_{22} \\ \sigma_{33} \\ \sigma_{12} \\ \sigma_{23} \\ \sigma_{13} \end{bmatrix} = \begin{bmatrix} a_{11} & a_{12} & a_{13} & 0 & 0 & 0 \\ a_{21} & a_{22} & a_{23} & 0 & 0 & 0 \\ a_{31} & a_{32} & a_{33} & 0 & 0 & 0 \\ 0 & 0 & 0 & a_{44} & 0 & 0 \\ 0 & 0 & 0 & 0 & a_{55} & 0 \\ 0 & 0 & 0 & 0 & 0 & a_{66} \end{bmatrix} \begin{bmatrix} \varepsilon_{11} \\ \varepsilon_{22} \\ \varepsilon_{33} \\ \varepsilon_{12} \\ \varepsilon_{23} \\ \varepsilon_{13} \end{bmatrix}$$

(2.1) will be written in the form

$$(2.2) \qquad \sigma = A\varepsilon.$$

In the case of the isotropic material we have in (2.1)

$$a_{11} = a_{22} = a_{33} = \lambda + 2\mu = \frac{(1-\nu)E}{(1+\nu)(1-2\nu)}$$

$$(2.3) \qquad a_{12} = a_{13} = a_{23} = a_{21} = a_{31} = a_{32} = \lambda = \frac{\nu E}{(1+\nu)(1-2\nu)}$$

$$a_{44} = a_{55} = a_{66} = 2\mu = \frac{E}{1+\nu} .$$

λ, μ are the Lamé constants, E is the modulus of elasticity, ν is the Poisson's ratio, and

$$\lambda = \frac{\nu E}{(1+\nu)(1-2\nu)} \qquad \mu = \frac{E}{2(1+\nu)}$$

Further we let

$$(2.4) \qquad \varepsilon^A(u) = \frac{1}{2} \int_\Omega \left[\sum_{i,j=1}^{3} \sigma_{ij} e_{ij} \right] dx$$

$$= \frac{1}{2} \int \left(\sigma_{11}e_{11} + \sigma_{22}e_{22} + \sigma_{33}e_{33} + 2\sigma_{12}e_{12} + 2\sigma_{23}e_{23} + 2\sigma_{13}e_{13} \right) dx$$

be the *strain energy* expression. We use the notation $\varepsilon^A(u)$ to emphasize that (2.4) is based on A given by (2.1). By the *total energy* we denote as usual

$$(2.5) \qquad G^A(u) = \varepsilon^A(u) - Q(u)$$

where

$$(2.6) \qquad Q(u) = \int_\omega \frac{q}{2} \left(u_3(x_1, x_2, \frac{d}{2}) + u_3(x_1, x_2, -\frac{d}{2}) \right) dx$$

The exact solution u of the plate problem *is the minimizer* of the total energy over the set of functions $\mathcal{H}(\Omega) \subset (H^1(\Omega))^3$ where $\mathcal{H}(\Omega)$ constrains

$(H^1(\Omega))^3$ on S (not on $R_{\pm}$). The boundary conditions of the plate problem are then uniquely characterized by the set $\mathcal{H}(\Omega)$.

3. The hierarchic family of plate models.

By the *plate model* we mean a *two-dimensional* boundary value problem which approximates the solution of the *three-dimensional* plate problem (defined in Section 2). By the hierarchic family of plate models we understand a *sequence* of models which solutions converge to the exact (three-dimensional) solution of the plate model and any model of the sequence converges (after scaling) as $d \longrightarrow 0$ to the same limit.

The plate model from the hierarchic family is defined as the minimizer $u^{(n)}$ of the quadratic functional

$$G^B(u) = \varepsilon^B(u) - Q(u) \tag{3.1}$$

over the set $\mathcal{H}(n) \subset \mathcal{H}(\Omega)$ of the functions of the form

$$u_i^{(n)}(x) = \sum_{j=0}^{n_i} u_{ij}^{(n)}(x_1, x_2)(x_3)^j, \qquad i = 1,2,3 \tag{3.2}$$

$n = (n_1, n_2, n_3)$ and B is certain compliance matrix depending on n, which could be different from A. The solution based on (3.1) and (3.2) will be called the solution of the n-model.

Because of the assumptions about the symmetry of the load we made in Section 2 we can assume

$$u_{1j} = u_{2j} = 0 \qquad \text{for } j \text{ even}$$

and

$$u_{3j} = 0 \qquad \text{for } j \text{ odd.}$$

Often, instead of (3.2),

$$u_i^{(n)}(x) = \sum_{j=0}^{n_i} u_{ij}^{(n)}(x_1,x_2)P_j\left[x_3\frac{2}{d}\right] \tag{3.2a}$$

is used. Here P_j is the Legendre polynomial of degree j. The solution $u^{(n)}$ using (3.2) or (3.2a) is the same because the span is the same. Form (3.2a) is preferable especially when adaptive approaches are used.

Finally by $\mathcal{H}^k \subset \mathcal{H}$ we denote the set of functions of the form

$$\begin{aligned} u_i(x_1,x_2,x_3) &= -\frac{\partial u_3}{\partial x_i}x_3, \qquad i = 1,2 \\ u_3(x_1,x_2,x_3) &= u_3(x_1,x_2) \end{aligned} \tag{3.3}$$

with $u_3(x_1,x_2) \in H^2(\omega)$. Function u^k is then the minimizer of the quadratic functional (3.1) over $\mathcal{H}^k$ (when using matrix B which will be specified later).

It is obvious that the set $\mathcal{H}(n)$ is dense in $\mathcal{H}(\Omega)$ as $n_i \longrightarrow \infty$, $i = 1,2,3$ and hence ${}^A u^{(n)} \longrightarrow u$ as $n_i \longrightarrow \infty$, $i = 1,2,3$ with the convergence in the energy norms. By index A in ${}^A u^{(n)}$ we indicate that the matrix A in (3.1) is used.

There is a vast amount of literature devoted to the derivation of various plate models. We refer here to [1,3,4] and references therein.

4. The problem of the simply supported, uniformly loaded (q(x)=1) plate.

In this section we still analyze various features of the plate problem when the *simple support*, which is the typical one in engineering analysis, is imposed at the boundary. In Section 5 we will address the plate problem with some other boundary conditions and discuss the properties of its solution in

comparison with the solution of simply supported plates.

4.1 The (three-dimensional) plate problem and the basic properties of its solution.

In this section we will address the three-dimensional plate problem and the properties of its solution. The solution will serve as the basis for the assessment of the accuracy of various plate models.

The simple support is an *idealization* which has no standard definition in the three-dimensional setting. We will consider here *only two different types* of simple supports:

α) the soft simple support

β) the hard simple support.

The *soft simple support* is characterized by the set $\mathcal{H}^S(\Omega) = \{u \in (H^1(\Omega))^3 \mid u_3 = 0 \text{ on } S\}$ and the *hard simple support* is characterized by the set $\mathcal{H}^H(\Omega) = \{u \in (H^1(\Omega))^3 \mid u_3 = 0, \ u_t = 0 \text{ on } S\}$. Here by u_t we denote the displacement in the tangential direction on Γ, i.e. $u_t = u_1 t_1 + u_2 t_2$ where $t = (t_1, t_2)$ is the unit tangent to Γ. In the vertices of ω (ω is assumed to be a polynomial domain) no constraint condition is prescribed. Because $u \in (H^1(\Omega))^3$ the constraint is interpreted in the usual trace sense.

The basic physical interpretation of both boundary conditions is obvious. In the case of the soft support, no tangential shear stresses are present, while in the case of hard support the tangential stresses lead to the twist moment reaction.

Let us first discuss the differences between the two mentioned cases of simple support for d small.

Theorem 4.1. Let u_d^S and u_d^H be the solution of the plate problem with the thickness d for the soft and hard support cases, respectively. Then

$$(4.1) \qquad \left[\frac{\varepsilon^A(u_d^S - u_d^H)}{\varepsilon^A(u_d^S)}\right]^{1/2} \longrightarrow 0 \qquad \text{as} \quad d \longrightarrow 0$$

The proof follows by arguments used in [2] [6]. □

Because $\mathcal{K}^S \supset \mathcal{K}^H$ we have $\varepsilon^A(u_d^S) \geq \varepsilon^A(u_d^H)$ and $\left[\varepsilon^A(u_d^S - u_d^H)\right]^{1/2} = \left[\varepsilon^A(u_d^S) - \varepsilon^A(u_d^H)\right]^{1/2}$. Theorem 4.1 shows that the difference between both supports measured in the (relative) energy norm converges to zero as $d \longrightarrow 0$. It is necessary to underline that this holds for the energy norm and not for all other norms as will be seen later. The main difference between the two supports is the behavior of the *solution in the neighborhood of* S. The size of this neighborhood depends on the relation between the plate thickness d and the smoothness of Γ. The following example shows that.

Let us consider ω_m to be a regular m-gon inscribed in the unit circle C as shown in Figure 4.1.

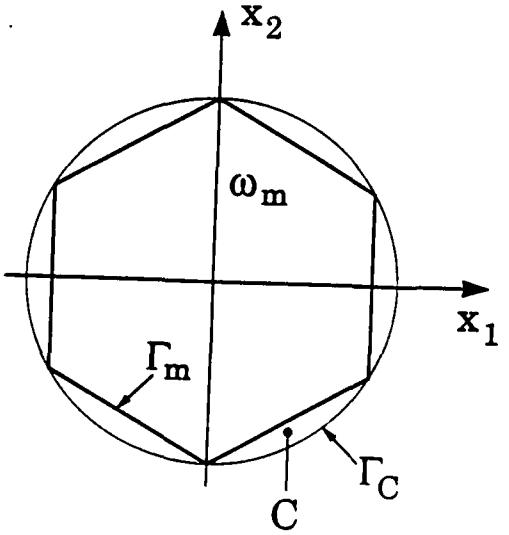

Figure 4.1. Scheme of the m-gon ω_m, (m = 6).

Denote by $u^H_{d,m}$ and $u^S_{d,m}$, respectively, the (three-dimensional) solution for the hard and soft support for the m-eck ω_m. By $u^H_{d,c}$ and $u^S_{d,c}$ we denote the solution on $C \times \left[-\frac{d}{2}, \frac{d}{2}\right]$ where on $\Gamma_c \times \left[-\frac{d}{2}, \frac{d}{2}\right]$ the hard and soft supports, respectively, are imposed. The solution is defined analogously as the minimizer of the energy over $\mathcal{H}^H$ or $\mathcal{H}^S$. We then have

Theorem 4.2. For any $0 < d < d_0$,

$$\lim_{m\to\infty} u^S_{d,m} \longrightarrow u^S_{d,c}$$

$$\lim_{m\to\infty} u^H_{d,m} \longrightarrow \tilde{u}_{d,c} \neq u^H_{d,c}$$

The convergence is understood in the energy norm on Ω_m. For the proof see

[6]. □

It is possible to compute the value

$$\xi(\nu) = \lim_{d\to 0} \lim_{m\to\infty} \frac{|u^S_{m,d}(0,0,0) - u^H_{m,d}(0,0,0)|}{|u^S_{m,d}(0,0,0)|},$$

$$\xi(0.3) = 0.264$$

(We have $\lim_{m\to\infty} |u^S_{m,d}(0,0,0)| > \lim_{m\to\infty} |u^H_{m,d}(0,0,0|)$

Theorem 4.2 shows that when m is large with respect to d^{-1} then the neighborhood of S where there is significant difference between hard and soft support solution can "fill" the entire Ω.

The boundary of the plate Ω has edges and vertices. Local behavior of the solution of the plate problem in the neighborhood of these edges and vertices is well-known. See for example [7] and [8].

Let us consider first the *horizontal* singularity. To this end let us assume that Γ_1 is a side of the polygon ω and $\Gamma_1 = \{x_1, x_2 \mid |x_1| < a, x_2 = 0\}$. Then the (horizontal) edge is $E_1 = \{x_1, x_2, x_3 | (x_1, x_2) \in \Gamma_1 \quad x_3 = \frac{d}{2}\}$. In the neighborhood of E_1 we have

$$
\begin{aligned}
u_1(x_1, x_2, x_3) &= \qquad\qquad + \text{ smoother term} \\
u_2(x_1, x_2, x_3) &= C(x_1) r_1^{\lambda} \phi_2(\theta) + \text{ smoother term} \\
u_3(x_1, x_2, x_3) &= C(x_1) r_1^{\lambda} \phi_3(\theta) + \text{ smoother term}
\end{aligned} \tag{4.2}
$$

where (r_1, θ) denotes the polar coordinates in the plane x_2, x_3 with the origin in E_1. Functions ϕ_2 and ϕ_3 are analytic in θ and function $C(x_1)$ is smooth on (open) interval $-a < x_1 < a$. In (4.2), the smoother term means a function which is smoother in the neighborhood of E_1 than the functions $r^{\lambda}\phi_i(\theta)$, $i = 2,3$. For the hard and soft support we have $\lambda = 0.71117$ (independently of the Poisson's ratio ν). Because $\lambda < 1$, the stresses are unbounded in the neighborhood of E_1. Nevertheless the moments

$$
M_{ij}(x_1, x_2) = \int_{-d/2}^{d/2} \sigma_{ij} x_3 \, dx_3, \qquad i, j, = 1,2 \tag{4.3}
$$

and the shear forces

$$
Q_{3,i}(x_1, x_2) = \int_{-d/2}^{d/2} \sigma_{ij} \, dx_3, \qquad i = 1,2 \tag{4.4}
$$

are bounded in the neighborhood of Γ_i (except possibly the vertices of Γ_i).

Consider now the *vertical* edge E_2. $E_2 = \{x_1 = 0, \; x_2 = 0, \; |x_3| < \frac{d}{2}\}$ when we assumed that the vertex of ω lies in the origin. We will assume that the internal angle at this vertex is α, $0 < \alpha \leq 2\pi$. In the

neighborhood of E_2 we have

$$
\begin{aligned}
u_1(x_1,x_2,x_3) &= C_1(x_3)r_2^{\lambda_1}\phi_1(\theta) + \text{ smoother term} \\
u_2(x_1,x_2,x_3) &= C_1(x_3)r_2^{\lambda_1}\phi_2(\theta) + \text{ smoother term} \\
u_3(x_1,x_2,x_3) &= C_2(x_3)r_2^{\lambda_2}\psi(\theta) + \text{ smoother term}
\end{aligned} \tag{4.5}
$$

Here (r_2,θ) are the polar coordinates in the x_1,x_2 plane, $\phi_i(\theta)$ and $\psi(\theta)$ are analytic in θ, and $C_1(x_3)$ and $C_2(x_3)$ are smooth on $\left[-\frac{d}{2}, \frac{d}{2}\right]$ with possible singular behavior at $\pm\frac{d}{2}$.

Coefficients λ_1 and λ_2 and functions ϕ_i, ψ depend on α and the type of boundary conditions. Coefficient λ_1 can be complex. Then there is a pair of conjugate coefficients because (4.5) has to be real.

$$
\begin{aligned}
u_1(x_1,x_2,x_3) = {} & C_1(x_3)r_2^{Re\lambda_1}\sin(\mathcal{I}_m Im\,\lambda_1 lgr)\,\phi_1(\theta) \\
& + \hat{C}_1(x_3)r_2^{Re\lambda_1}\cos(\mathcal{I}_m Im\,\lambda_1 lgr)\,\hat{\phi}_1(\theta) \\
& + \text{smoother terms}
\end{aligned}
$$

and analogously $u_2(x_1,x_2,x_3)$.

The coefficients λ_1,λ_2 can be integers or they can be of multiplicity >1 for some angles α. Then these angles are exceptional and in general the term r^{λ} has to be replaced by $r^{\lambda}(lgr)^S$, S an integer. Only a finite number of exceptional angles exist. In the neighborhood of these exceptional angles the singular behavior is not continuous with respect to the α. We will not address here these cases although they will also occur in some of our examples.

In Table 4.1 we show the values of λ_1 and λ_2 in (4.5) for hard and soft supports for various angles α. They are independent of the Poisson's

ratio ν. We see that the angles $\alpha = 30^\circ, 45^\circ, 90^\circ$ are exceptional because λ_2 is an integer. The angle 360° leads to the multiplicity two. For α = 30-135 the coefficient λ_1 in the table for the soft support case are complex. For more see [9].

Table 4.1 The coefficients λ_1 and λ_2 in (4.5) for the hard and soft support.

α	λ_1		λ_2	
	HARD	SOFT	HARD	SOFT
30	3.4846	8.0630 + i 4.2028	6.0000	6.0000
45	2.4129	5.3905 + i 2.7204	4.0000	4.0000
90	1.4208	2.7396 + i 1.1190	2.0000	2.0000
120	1.2048	2.0941 + i 0.6046	1.5000	1.5000
135	1.1368	1.8853 + i 0.3606	1.3333	1.3333
150	1.0832	1.5339	1.2000	1.2000
225	0.7263	0.6736	0.8000	0.8000
270	0.5951	0.5445	0.6667	0.6667
315	0.5330	0.5050	0.5714	0.5714
360	0.5000	0.5000	0.5000	0.5000

We see that for some angles we have $\lambda < 1$ and hence in these cases the stresses are unbounded as $r_2 \longrightarrow 0$. We have then

$$(4.6)\quad M_{ij} = C_1 r_2^{\lambda_1 - 1}\phi_{ij}(\theta) + \text{smoother terms}, \qquad i,j = 1,2$$

$$(4.7)\quad Q_{3j} = C_2 r_2^{\lambda_2 - 1}\phi_j(\theta) + \text{smoother terms}, \qquad j = 1,2$$

We mention that the expressions (4.6) and (4.7) do not follow directly from (4.5) because the solution has other singularities in the vertex and also $C_1(x_3)$ in (4.5) can be singular for $x_3 = \pm\frac{d}{2}$. Nevertheless these singularities are weaker and do not influence the form (4.6) (4.7).

The expressions (4.6) and (4.7) show that the moments and shear forces in the neighborhood of the vertex of ω can be unbounded. For example, this happens when ω is an L-shaped domain and $\alpha = 270^\circ$. The shear forces have the same strength of the singularity for the hard and soft support, while the singularity of the moments is different for the hard and soft support. Furthermore, the singular behavior is different for the moments and shear forces. The mentioned behavior described by (4.6) and (4.7) is valid only for $r \ll d$ as will be seen later in Section 4.5.

It is interesting to mention that the differences in the singular behavior of the hard and soft supports do not explain Theorem 4.2, whose proof is based on completely different principles.

4.2 The (three-dimensional) problem of a simply supported, uniformly loaded square plate. Numerical results.

In this section we will present numerical results of the analysis of the square plate.

Let $\omega = \{x_1, x_2 \mid |x_1| < 0.5, \quad |x_2| < 0.5\}$ and let $d = \frac{1}{100}$ and consider the three-dimensional problem with $\nu = 0.3$. In this case $\alpha = 90^\circ$ and hence from Table 4.1 we conclude that the moments and shear forces are bounded and are sufficiently smooth up to the boundary.

The main question we will consider in this section is the difference between the solution when the hard and soft simple support is prescribed on S. The solution is obviously symmetric with respect to the axes x_1 and x_2 and hence only a quarter of the plate will be considered.

First we consider the behavior of the twist moment $M_{12}(x_1,x_2)$ for $x_1 = 0.4$, $x_1 = 0.5$ as a function of the variable x_2. Denoting M_{12}^H and M_{12}^S, respectively, the twist moments for the hard and soft support, we have $M_{12}^S(x_1, 0.5) = 0$ while $M_{12}^H(x_1, 0.5) \neq 0$. This indicates that the boundary layer has to be present because of Theorem 4.1 which shows that the difference of both solutions converges to zero as $d \longrightarrow 0$.

In Table 4.2 we show the values of the twist moment $M_{12}(x_1,x_2)$. We clearly see that the boundary layer is of order d.

Table 4.2 The twist moment $M_{12}(x_1,x_2)$ $x_1 = 0.4, 0.5$ for the hard and soft support.

x_2	$x_1 = 0.4$		$x_1 = 0.5$	
	HARD	SOFT	HARD	SOFT
0.0	0.	0.	0.	0
0.02368	0.0018	0.0019	0.0020	0
0.11842	0.0092	0.0092	0.0097	0
0.21316	0.0162	0.0163	0.0172	0
0.45000	0.0289	0.0292	0.0315	0
0.48079	0.0294	0.0297	0.0323	0
0.49026	0.0295	0.0285	0.0324	0
0.49500	0.0295	0.0237	0.0325	0
0.49713	0.0295	0.0179	0.0325	0
0.49903	0.0295	0.0080	0.0325	0
0.49950	0.0295	0.0045	0.0325	0
0.50000	0.0295	0.	0.0325	0

Remark. The exact solution is not known. Nevertheless the data we report are reliable. They were computed by refined meshes, and high degree elements with an analysis of the accuracy.

Figure 4.2 shows $M_{12}^{H}(0.4, x_2)$ with $\max M_{12}^{H}(0.4, x_2) = 0.0295$ and $M_{12}^{S}(0.4, x_2)$ with $\max M_{12}^{S}(0.4, x_2) = 0.0297$.

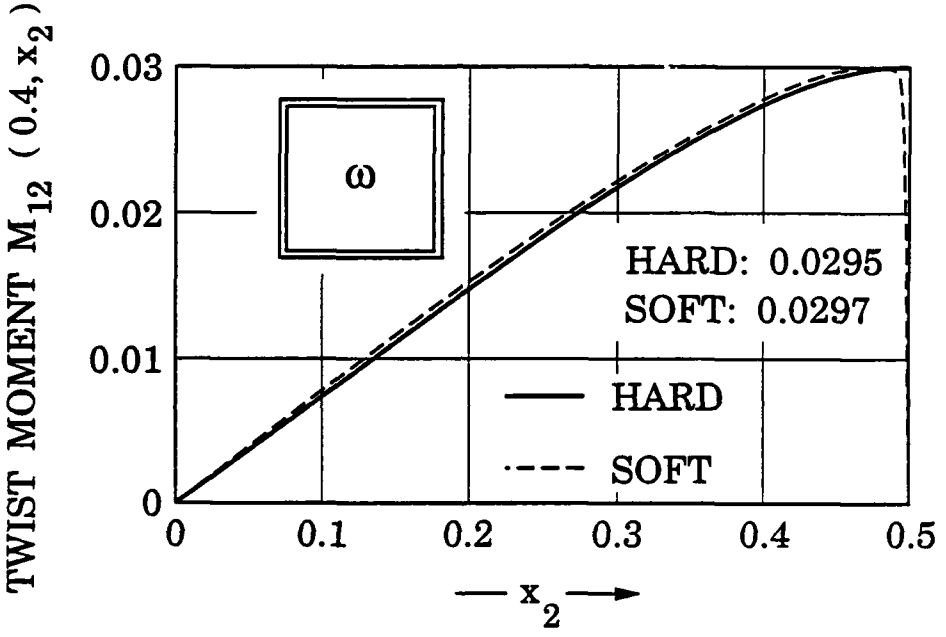

Figure 4.2. The moments $M_{12}^{H}(0.4, x_2)$ and $M_{12}^{S}((0.4, x_2)$ for the 3-dimensional problem.

The shear forces $Q_{3j}(x_1, x_2)$, $j = 1,2$ show the similar boundary layer we mention that $Q_{32}^{H}(x_1, 0.5) = 0$ while $Q_{32}(x_1, 0.5) \neq 0$.

Table 4.3. The shear force $Q_{3j}(x_1, x_2)$, $j = 1,2$, $x_1 = 0.4, 0.5$ for the hard and soft support.

x_2	$x_1 = 0.4$				$x_1 = 0.5$			
	Q_{31}		Q_{32}		Q_{31}		Q_{32}	
	HARD	SOFT	HARD	SOFT	HARD	SOFT	HARD	SOFT
0.0	0.2460	0.2446	0.	0.0	0.3373	0.4206	0.0	0.0
0.02368	0.2451	0.2445	0.0041	0.0041	0.3373	0.4206	0.0	-0.6433
0.11842	0.2347	0.2346	0.0215	0.0214	0.3260	0.4080	0.0	-3.1986
0.21316	0.2086	0.2086	0.0386	0.0386	0.2973	0.3740	0.0	-5.6633
0.45000	0.0526	0.0503	0.1274	0.1274	0.1073	0.1326	0.0	-10.4513
0.48079	0.0207	-0.0046	0.1526	0.1526	0.0534	-0.1334	0.0	-10.6353
0.49026	0.0107	-0.4193	0.1606	0.1633	0.0306	-0.8126	0.0	-9.9046
0.49500	0.0053	-1.9206	0.1660	0.1760	0.0184	-2.1746	0.0	-8.6002
0.49713	0.0030	-3.7753	0.1680	0.1880	0.0133	-3.5240	0.0	-7.7056
0.49903	0.0012	-6.9740	0.1701	0.2066	0.0038	-5.4623	0.0	-6.9546
0.49950	0.0005	-8.1673	0.1706	0.2133	0.0019	-6.0693	0.0	-6.8382
0.50000	0.0	-9.7186	0.1713	0.2213	0.0	-6.7933	0.0	-6.7933

In Figures 4.3 and 4.4 we show $Q_{13}(0.5, x_2)$ (= reaction) and $Q_{23}(0.5, x_2)$ for the soft support.

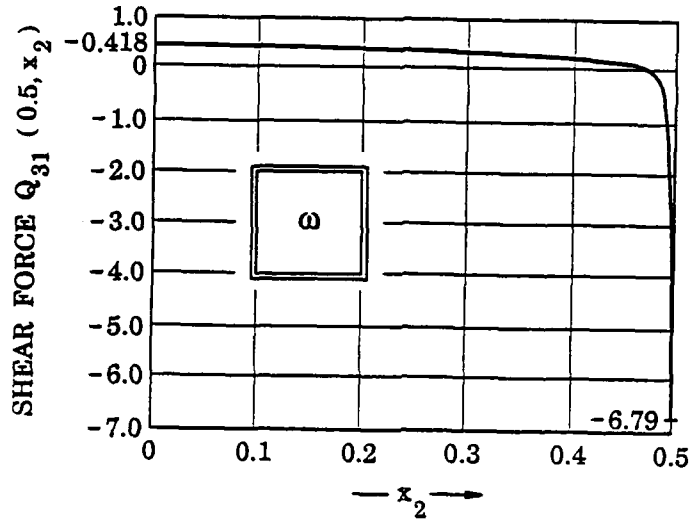

Figure 4.3. The shear force $Q_{31}(0.5, x_2)$ for the soft support (three-dimensional problem).

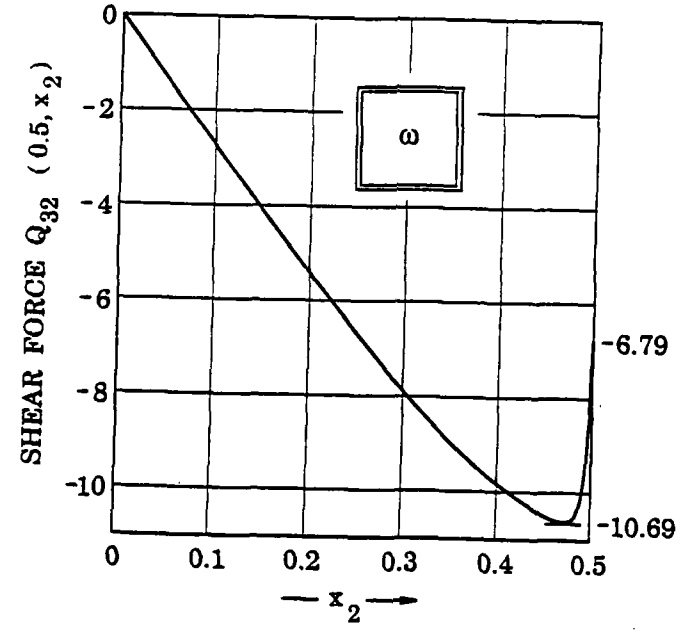

Figure 4.4. The shear force $Q_{32}(0.5, x_2)$ for the soft support (three-dimensional problem).

Tables 4.2, 4.3 and Figures 4.2, 4.3, and 4.4 show that the difference between hard and soft support resides in the boundary layer behavior. The hard support does not have a boundary layer and can serve as a smooth extension to the boundary. To understand the boundary layer more precisely we let

$$\left| \frac{M_{12}^{H}(x_1, x_2) - M_{12}^{S}(x_1, x_2)}{M_{12}^{H}(x_1, 0.5)} \right| = \exp\left[-\beta_{12}(x_1, x_2) \frac{(0.5 - x_2)}{d} \right]$$

and

$$\left| \frac{Q_{31}^{H}(x_1, x_2) - Q_{31}^{S}(x_1, x_2)}{Q_{3,1}^{H}(x_1, 0.5)} \right| = \exp\left[-\beta_{31}(x_1, x_2) \frac{(0.5 - x_2)}{d} \right]$$

Table 4.4 shows some values of $\beta_{12}(x_1, x_2)$ and $\beta_{31}(x_1, x_2)$.

Table 4.4 The functions $\beta_{12}(x_1, x_2)$ and $\beta_{31}(x_1, x_2)$.

x_2	$\beta_{12}(x_1, x_2)$		$\beta_{31}(x_1, x_2)$		
	$x_1 = 0.4$	$x_1 = 0.49$	$x_1 = 0.4$	$x_1 = 0.49$	$x_1 = 0.5$
0.49263	3.34	2.74	3.22	3.72	2.17
0.49500	3.28	3.10	3.24	3.53	2.27
0.49666	3.26	3.18	3.28	3.53	2.28
0.49878	3.27	3.30	3.40	3.62	2.23
0.49950	3.31	3.34	3.51	3.73	2.22
0.49989	3.46	3.49	3.62	3.84	2.22
0.49991	3.52	3.54	3.63	3.84	2.21
0.49994	3.62	3.64	3.63	3.84	2.21

In Figure 4.5 we show the function β_{31} and in Figure 4.6 we show the β_{12}. We see that the β_{31} and β_{32} increases when $x_2 \rightarrow 0.5$. This is typical for the three-dimensional formulation where essentially infinite number of

boundary layers are present but here only the first one is visible. Also typical is the discontinuity of $\beta_{31}(x_1, x_2)$ when $x_1 \longrightarrow 0.5$. We see that for $x_1 = 0.5$ the value of β_{31} is significantly smaller than for $x_1 = 0.49$.

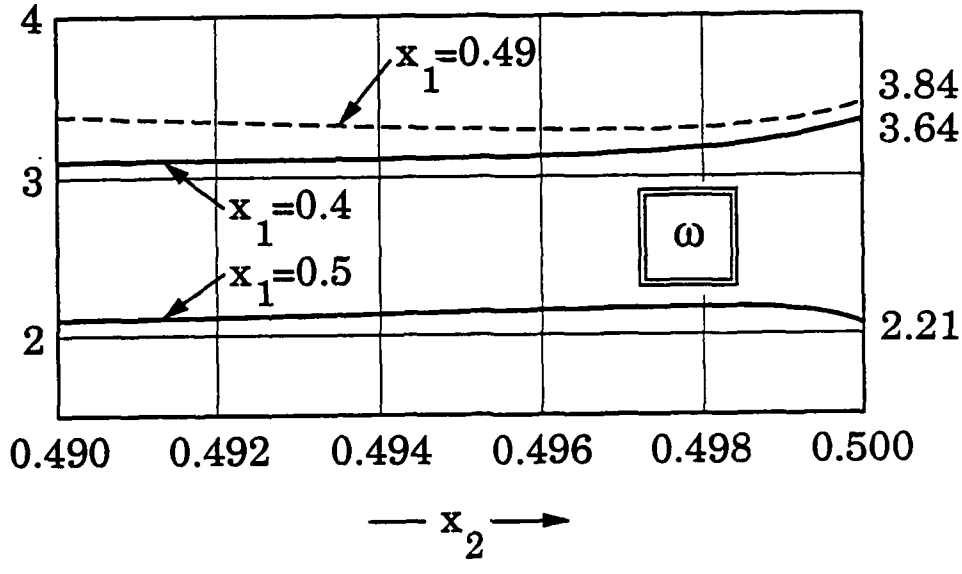

Figure 4.5. The function $\beta_{31}(x_1, x_2)$ for $x_1 = 0.4,\ 0.49,\ 0.5$ (three-dimensional formulation).

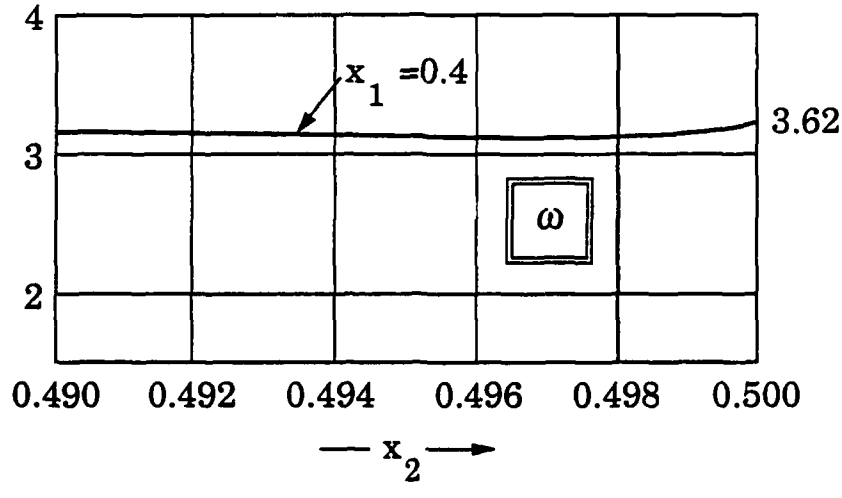

Figure 4.6. The function $\beta_{12}(x_1, x_2)$ for $x_1 = 0.4$ (three-dimensional formulation).

The shear force $Q_{31}(0.5, x_2)$ is the reaction of the plate. We see from Fig. 4.3 and Table 4.3 that for the soft support this reaction is negative in the neighborhood of the vertex $x_2 \approx 0.5$. This relates to a well-known effect in the Kirchhoff theory (see Section 4.6). It is interesting to define

$$\mathcal{R} = \int_I Q_{31}(0.5, x_2)\, dx_2$$

where $I = \{0 < x_2 < 0.5 \mid Q_{31}(0.5, x_2) \leq 0\}$. We get in our case $\mathcal{R} = 0.0290$.

The data we present here are for $d = \frac{1}{100}$. $Q_{3,1}(0.5, 0.5)d \to \bar{Q}_{3,1}(0.5, 0.5)$, as $d \longrightarrow 0$ where $\bar{Q}_{3,1}$ is a certain value which we expect to be approximately 0.068, although the authors do not know whether a rigorous proof of it exists. Analogously $\mathcal{R} \longrightarrow \bar{\mathcal{R}}$ as $d \longrightarrow 0$. We expect that $\bar{\mathcal{R}} \approx 0.029$ which is different from the value 0.0325 arising from the Kirchhoff model (see Section 4.6).

The boundary layer is also visible in the energy of the solution. We have in our case $d = \frac{1}{100}$

$$\left[\frac{\varepsilon^A(u^H)}{\varepsilon^A(u^S)}\right]^{1/2} = 0.895$$

and hence the difference between hard and soft support measured in the energy norm is 9%. Of course as $d \longrightarrow 0$ the energy norm of this difference converges to zero due to Theorem 4.1. We discussed only the square plate here. If the plate is rhombic then the difference between the hard and soft support increases.

4.3 The dimensionally reduced models.

We will consider here the n-model introduced in Section 3 which is based on the minimization of the quadratic functional $G^B(u)$ given in (3.1) over

the set of all functions of the form (3.2) constrained in the space $\mathcal{H}(\Omega)$.

We have now:

Theorem 4.3. Let $n = (n_1, n_2, n_3)$, $n_1 \geq 1$, $n_2 \geq 1$, $n_3 \geq 2$. Denoting by $A_{u_d}^{(n)}$ the plate model based on (3.1) (3.2) with $B = A$ (A given by (2.1) (2.3)) then for both types of simple support we have

$$(4.8) \qquad \frac{\varepsilon^A(A_{u_d}^n - u_d)}{\varepsilon^A(u_d)} \longrightarrow 0 \qquad \text{as} \quad d \longrightarrow 0$$

The proof follows by using arguments in [6]. □

The assumption that $n_3 \geq 2$ in Theorem 4.3 is essential. If $n_3 = 0$ and $\nu = 0$ then (4.8) still holds but when $\nu > 0$ (4.8) does not hold. This means that the case $n_3 = 0$ with the matrix A cannot be used except when $\nu = 0$. Hence the following problem arises: Find a class $\mathcal{B}$ of matrices B which when used instead of A leads to

$$(4.8a) \qquad \left[\frac{\varepsilon^A(B_{u_d}^n - u_d)}{\varepsilon^A(u_d)}\right]^{1/2} \longrightarrow 0 \qquad \text{as} \quad d \longrightarrow 0$$

Here by $B_{u_d}^n$ we denoted the minimizer of (3.1) with $n = (1,1,0)$ and matrix B instead of A.

The class $\mathcal{B}$ which guarantees (4.8a) is the class of matrices (4.9).

$$(4.9)\qquad B = \begin{bmatrix} \frac{E}{1-\nu^2} & \frac{\nu E}{1-\nu^2} & 0 & 0 & 0 & 0 \\ \frac{E}{1-\nu^2} & \frac{E}{1-\nu^2} & 0 & 0 & 0 & 0 \\ 0 & 0 & \frac{E}{1-\nu^2} & 0 & 0 & 0 \\ 0 & 0 & 0 & \frac{E}{1+\nu} & 0 & 0 \\ 0 & 0 & 0 & 0 & \frac{E\mathcal{H}}{1+\nu} & 0 \\ 0 & 0 & 0 & 0 & 0 & \frac{E\mathcal{H}}{1+\nu} \end{bmatrix}$$

Here E and ν are the modulus of elasticity and the Poisson's ratio and $\mathcal{H} > 0$ is an arbitrary parameter. We have,

Theorem 4.4. Let $n = (1,1,0)$ and let $^{B}u^{n}$ be the minimizer of (3.1) (3.2) with the matrix B given by (4.9). Then for both types of simple support we have

$$(4.9)\qquad \left[\frac{\varepsilon^{A}(u_d - {}^{B}u_d^{n})}{\varepsilon^{A}(u_d)}\right]^{1/2} \longrightarrow 0 \qquad \text{as} \quad d \longrightarrow 0$$

The proof follows by the arguments used in [6]. □

The coefficient $\mathcal{H}$ in B does not influence the validity of (4.9) but it influences the size of the difference $^{B}u_d^{n} - u_d$. The solution $^{B}u_d^{n}$ ($n = (1,1,0)$) is the famous Reissner-Mindlin solution. The recommendation for the selection of $\mathcal{H}$ was made by various authors. In [10] the value 5/6 is recommended. In the connection with wave propagation in [11], suggested values range almost from 0.76 for $\nu = 0$ to 0.91 for $\nu = 0.5$. Another recommendation is made e.g. in [12]. $\mathcal{H}(0) = 0.833$, $\mathcal{H}(0.33) = 0.850$, $\mathcal{H}(0.5) = 0.87$. We will address this question later in the numerical way.

Let us mention that for any n-model with $n_3 \geq 2$, using the matrix B

will not lead to (4.9).

The n-model reproduces Theorem 4.2. We have,

Theorem 4.5. Let $n_3 \geq 2$ with using A or $n_3 = 0$ using B. Then for any $d \leq d_0$

$$\lim_{m \to \infty} u_{d,n}^{(n)S} \longrightarrow u_{d,c}^{(n)S}$$

$$\lim_{m \to \infty} u_{d,n}^{(n)H} \longrightarrow \tilde{u}_{d,c}^{(n)} \neq u_{d,c}^{(n)}$$

For the proof, again see [6]. □

Using matrix B and (3.3) together with (3.1) (3.2) we obtain the Kirchhoff solution u_d^k and

Theorem 4.6. We have

$$(4.10) \qquad \left[\frac{\varepsilon^A(u_d - u_d^k)}{\varepsilon^A(u_d)}\right]^{1/2} \longrightarrow 0 \qquad \text{as} \quad d \longrightarrow 0$$

See [6] for proof. □

The Kirchhoff model cannot distinguish between the soft and hard support (see Section 4.6 for more) and the second part of Theorem 4.2 holds for the Kirchhoff model too. Various paradoxical properties of Kirchhoff model for simple support were discussed in [6,13,14].

The n-model solution has a boundary layer. In [15] and [16] the boundary layer of the Reissner-Mindlin solution was rigorously analyzed in detail when ω has smooth boundary. The rigorous analysis of the boundary layer structure of the solution for a domain ω with piecewise smooth boundary is not available. For additional analyses see also [17]. The solution from the Kirchhoff model has no boundary layer.

From (4.9) and (4.10) it follows that the Reissner-Mindlin solution con-

verges in energy to the Kirchhoff model. Nevertheless we underline that this is only in the energy. At the boundary the convergence does not occur. Using the analytical results in [15] for infinite half-plane this can be easily analytically demonstrated.

In Section 4.2 we analyzed the singular behavior of the plate solution in the neighborhood of the corners of the domain. We especially addressed in (4.6) (4.7) the singularity of M_{ij} and Q_{ij} as functions of internal angle α. The Reissner-Mindlin model, n-model, and Kirchhoff model solution also lead to the singular behavior of M_{ij} and Q_{ij}. The forms (4.6) (4.7) are also valid here, i.e. we have

$$M_{ij} = C_1 r_2^{\lambda_1^{(n)}-1} \phi_{ij}(\theta) + \text{smoother terms}, \qquad i,j = 1,2$$

$$Q_{3j} = C_2 r_2^{\lambda_2^{(n)}-1} \phi_j(\theta) + \text{smoother terms}, \qquad j = 1,2$$

In general $\lambda_i^{(n)}$ depends on n, i.e. on the model, and they are different for different models and for different types of boundary conditions. In Table 4.1 we gave the values of λ_i, $i = 1,2$ for the three-dimensional problem. In Table 4.5 we list the coefficients λ_1 for the n-models and Kirchhoff model for the soft support and hard support analogously to Table 4.1. We mention that the Kirchhoff model does not distinguish between the hard and soft support.

Table 4.5 The coefficients λ_1 and λ_2 for the hard and soft for various models.

α	λ_1				λ_2	
	HARD		SOFT	K	HARD SOFT	K
	RM	(1,1,2) 3 dim	RM, (1,1,2) 3 dim		RM, (1,1,2) 3 dim	
30	3.7972	3.4846	8.0630 + i 4.2028	5.0000	6.0000	4.0000
45	2.6083	2.4129	5.3905 + i 2.7204	3.0000	4.0000	2.0000
90	1.4905	1.4208	2.7396 + i 1.1190	1.0000	2.0000	0.0000
120	1.2404	1.2048	2.0941 + i 0.6046	0.5000	1.5000	-0.5000
135	1.1609	1.1368	1.8853 + i 0.3606	0.3333	1.3333	-0.6666
150	1.0978	1.0832	1.5339	0.2000	1.2000	-0.8000
225	0.7354	0.7263	0.6736	0.2000	0.8000	-0.8000
270	0.6040	0.5951	0.5445	0.3333	0.6667	-0.6667
315	0.5379	0.5330	0.5050	0.1428	0.5741	-0.8572
360-0	0.5000	0.50000	0.5000	0.0000	0.5000	-1.0000

For $\alpha = 360^\circ$ we list the limiting value $\alpha = 360\text{-}0$ which is not equal to the value $\alpha = 360^\circ$. We see that for the hard support the Reissner-Mindlin model and (1,1,2) model give slightly different values while the Kirchhoff model yields very different singularity coefficients. For the formula for these values we refer to [9].

4.4. The n-model of simply supported uniformly loaded square plate. Numerical results.

In this section we consider the same problem as in Section 4.2 namely

the square plate $d = \frac{1}{100}$, $\nu = 0.3$ and soft and hard simply support. Further we will assume that $E = 10^7$.

As we mention in Section 4.3 the Reissner-Mindlin model $(n = (1,1,0))$ depends on the value of the parameter $\mathcal{H}$. Let us first show the dependence of the energy $\varepsilon(\mathcal{H})$ (of the quarter of the plate) on the value of $\mathcal{H}$ for various models. Denote further the quantity

$$\varepsilon = \left[\frac{|\varepsilon(\mathcal{H}) - \varepsilon(3\ \mathrm{dim})|}{|\varepsilon(3\ \mathrm{dim})|}\right]^{1/2}.$$

The values of $\varepsilon(\mathcal{H})$ and ε for the soft support is shown in Table 4.6.

We see that by using different values of the parameter $\mathcal{H}$, the energy of the RM model can be over or under the true 3-dimensional energy. The energy in the case $(1,1,2)$ is smaller than the energy of the RM solution for $\mathcal{H} = 1$. If $\nu = 0$ then for $\mathcal{H} = 1$ we get $A = B$ and the energy of $(1,1,2)$ model would be larger than that of the RM model. It seems remarkable that the performance of RM model (for this particular case) is better for all $\frac{5}{6} \le \mathcal{H} \le 1$ than that of the model $(1,1,2)$ and $\mathcal{H} = 1$. This conclusion is not valid in general for all boundary conditions. The model $(3,3,4)$ $(\mathcal{H} = 1)$ gives then the better results than the RM model.

Table 4.6 Energy $\varepsilon(\mathcal{H})$ as a function of $\mathcal{H}$ and different plate models for the soft support

$\mathcal{H}$	$\varepsilon(\mathcal{H}) \times 10^3$	ε%	Model
1	0.234563	2.69	RM
0.91	0.234674	2.26	RM
0.87	0.234729	0.41	RM
0.845333	0.234765	1.16	RM
5/6	0.234783	1.46	RM
1	0.234528	2.95	(1,1,2)
1	0.234731	0.29	(3,3,4)
1	0.234732	0.01	(5,5,6)
0.87	0.234693	1.3	(1,1,2)
0.87	0.234913	2.76	(3,3,4)
0.87	0.234914	2.78	(5,5,6)
Kirchhoff	0.232392	9.98	K
3 dim	0.234735	——	——

Table 4.6 has addressed the soft support. Table 4.7 addresses the hard support.

Table 4.7 The energy for the various models for the hard support.

$\mathcal{H}$	$\varepsilon \times 10^3$	ε%	Model
0.87	0.232524	1.22	RM
1	0.232472	0.85	(1,1,2)
1	0.232489	0.01	(3,3,4)
1	0.232489	——	(5,5,6)
Kirchhoff	0.232392	2.04	K
3 dim	0.232489	——	——

We see that for hard support the performance of the model (1,1,2), $\mathcal{K} = 1$ is better than of RM model with $\mathcal{K} = 0.87$, which is in contrast with the soft support. Let us also underline that the energy of RM model with $\mathcal{K} = 0.87$ is larger for hard support than that of the energy of the 3-dimensional solution. The same occurs for $\mathcal{K} = \frac{5}{6}$ and soft support.

In Table 4.6 we also report the values of the (n_1, n_2, n_3) model when $a_{44} = a_{55} = \frac{\mathcal{K}E}{1 + \nu}$ with $\mathcal{K} = 1$ and $\mathcal{K} = 0.87$. We see that it is advantageous for the model (1,1,2) but detrimental for higher models compared with the solutions of the 3-dimensional plate model.

In Table 4.8 we show the value of the shear force Q_{31} on the diagonal $x_1 = x_2$ and the error when compared with the solution of the 3-dimensional plate model.

Table 4.8 The shear force Q_{31} and its error on the line $x_1 = x_2$ for the soft support.

$x_1 = x_2$	3 dim	$\mathcal{K} = 1$		$\mathcal{K} = 0.91$		$\mathcal{K} = 0.87$		$\mathcal{K} = 5/6$	
		Q_{31}	$\varepsilon\%$	Q_{31}	$\varepsilon\%$	Q_{31}	$\varepsilon\%$	Q_{31}	$\varepsilon\%$
0.4905	-0.29	-0.22	24.9	-0.26	11.9	-0.28	5.3	-0.29	0.92
0.4950	-1.55	-1.46	6.0	-1.52	2.3	-1.55	0.7	-1.57	0.77
0.4968	-2.78	-2.79	0.4	-2.80	0.8	-2.81	0.9	-2.81	0.81
0.4986	-4.75	-5.01	5.5	-4.87	2.6	-4.81	1.3	-4.75	0.07
0.49905	-5.37	-5.70	6.1	-5.51	2.5	-5.41	0.9	-5.33	0.76
0.49995	-6.70	-7.08	5.6	-6.77	0.9	-6.62	1.4	-6.49	3.31
0.5	-6.79	-7.16	5.5	-6.83	0.7	-6.68	1.4	-6.54	3.53

In what follows we always use in the RM model the value of $\mathcal{K} = 0.87$, unless otherwise stated.

In Tables 4.9a and 4.9b we show the moment M_{12} computed by the RM ($\mathcal{K} =$

0.87) and (1,1,2) ($\mathcal{H}$ = 1.00) model for the hard and soft support. Analogous results are given in Table 4.2 for the three-dimensional solution.

In the table we also show that relative error ε in comparison with the three-dimensional solution whenever it is larger than 0.1%. In the case of hard support, both RM and (1,1,2) models have error < 0.1%. It is interesting that the model (1,1,2) produces a larger error for the soft support moment M_{12} than the RM model. Model (3,3,4) would give better results than the RM model.

Table 4.9a The moment $M_{12}(x_1,x_2)$, x_1 = 0.4 for hard and soft support.

x_2	x_1 = 0.4					
	HARD		SOFT			
	RM	(1,1,2)	RM	ε_{RM}%	(1,1,2)	ε_{112}%
0.	0.	0.	0.	0.	0.	0.
0.02368	0.0018	0.0018	0.0018	0.	0.0018	0.
0.11842	0.0092	0.0092	0.0092	0.	0.0092	0.
0.21316	0.0162	0.0162	0.0163	0.	0.0163	0.
0.35526	0.0252	0.0252	0.0254	0.	0.0254	0.
0.45000	0.0289	0.0289	0.0292	0.	0.0292	0.
0.48079	0.0294	0.0294	0.0297	0.	0.0297	0.
0.49026	0.0295	0.0295	0.0286	0.3	0.0283	1.1
0.49500	0.0295	0.0295	0.0239	0.7	0.0246	3.4
0.49713	0.0295	0.0295	0.0180	0.9	0.0188	5.03
0.49903	0.0295	0.0295	0.0087	0.3	0.0085	6.3
0.49950	0.0295	0.0295	0.0045	0.	0.0047	6.0
0.50000	0.0295	0.0295	0.	0.	0.	0.

Table 4.9b The moment $M_{12}(x_1,x_2)$, $x_1 = 0.5$ for hard and soft support.

x_2	$x_1 = 0.5$			
	HARD		SOFT	
	RM	(1,1,2)	RM	(1,1,2)
0.	0.	0.	0.	0.
0.02368	0.0019	0.0019	0.	0.
0.11842	0.0097	0.0097	0.	0.
0.21316	0.0172	0.0172	0.	0.
0.35526	0.0270	0.0270	0.	0.
0.45000	0.0315	0.0315	0.	0.
0.48079	0.0323	0.0323	0.	0.
0.49026	0.0324	0.0324	0.	0.
0.49500	0.0325	0.0325	0.	0.
0.49713	0.0325	0.0325	0.	0.
0.49903	0.0325	0.0325	0.	0.
0.49950	0.0325	0.0325	0.	0.
0.50000	0.0325	0.0325	0.	0.

In Tables 4.10a and 4.10b we show analogous data for the shear forces.

Once more we see that for hard support the accuracy is high for RM and (1,1,2) model. Otherwise we see once more that the values are better for RM model ($\mathcal{H} = 0.87$) than for the (1,1,2) ($\mathcal{H} = 1$) model.

We will see in Section 5 that this conclusion is not necessarily correct for other boundary conditions.

Table 4.10a The shear forces $Q_{31}(x_1,x_2)$, $x_1 = 0.4$

x_2	$x_1 = 0.4$					
	Q_{31}					
	HARD		SOFT			
	RM	(1,1,2)	RM	ε_{RM}%	(1,1,2)	ε_{112}%
0.	0.246	0.246	0.246	0.	0.246	0.
0.02368	0.245	0.245	0.245	0.	0.245	0.
0.11842	0.234	0.234	0.234	0.	0.234	0.
0.21316	0.209	0.208	0.208	0.	0.208	0.
0.35526	0.134	0.134	0.134	0.	0.133	0.
0.45000	0.053	0.053	0.056	0.	0.055	0.
0.48079	0.021	0.021	0.001	—	0.006	—
0.49026	0.011	0.011	-0.403	3.8	-0.343	18.1
0.49500	0.005	0.005	-1.912	0.4	-1.822	5.1
0.49713	0.003	0.003	-3.817	1.1	-3.824	1.3
0.49903	0.001	0.001	-7.047	1.0	-7.379	5.8
0.49950	0.000	0.000	-8.214	0.3	-8.695	6.3
0.50000	0.	0.	-9.639	0.8	-10.323	6.3

Table 4.10b The shear forces $Q_{31}(x_1,x_2)$ and $Q_{32}(x_1,x_2)$, $x_1 = 0.5$

x_2	$x_1 = 0.5$							
	Q_{31}				Q_{32}			
	SOFT				SOFT			
	RM	ε_{RM}%	(1,1,2)	ε_{112}%	RM	ε_{RM}%	(1,1,2)	ε_{112}%
0.	0.419	0.	0.419	0.	0.	——	0.	——
0.02368	0.421	0.	0.421	0.	-0.638	0.8	-0.685	6.2
0.11842	0.408	0.	0.408	0.	-3.173	0.8	-3.399	6.2
0.21316	0.374	0.	0.374	0.	-5.617	0.8	-6.018	6.2
0.35526	0.273	0.	0.273	0.	-8.844	0.8	-9.474	6.2
0.45000	0.133	0.	0.135	1.5	-10.363	0.8	-11.095	6.2
0.48079	-0.125	——	-0.105	——	-10.559	0.6	-11.332	6.5
0.49026	-0.807	0.6	-0.756	6.9	-9.844	0.6	-10.651	7.5
0.49500	-2.188	0.6	-2.157	0.8	-8.505	1.1	-9.251	7.5
0.49713	-3.573	1.3	-3.645	3.4	-7.569	1.7	-8.221	6.6
0.49903	-5.499	0.6	-5.815	6.3	-6.881	1.9	-7.368	6.0
0.49950	-6.073	0.7	-6.485	6.5	-6.721	1.7	-7.252	6.4
0.50000	-6.678	1.5	-7.221	6.5	-6.678	1.5	-7.221	6.5

In Table 4.11 we show the values of $Q_{31}(0.5, 0.5)$ for soft support for various models.

Table 4.11 The value of $Q_{31}(0.5, 0.5)$ for soft support and various plate models.

$\mathcal{H}$	Q_{31}	ε%	Model
1	-7.15	5.6	RM
0.91	-6.83	0.8	RM
0.87	-6.68	1.5	RM
0.845333	-6.61	2.8	RM
5/6	-6.54	3.4	RM
1	-7.22	6.5	(1,1,2)
1	-6.82	0.6	(3,3,4)
1	-6.80	0.3	(5,5,6)
0.87	-6.73	0.9	(1,1,2)
0.87	-6.36	6.3	(3,3,4)
0.87	-6.34	6.6	(5,5,6)
3 dim	-6.97	——	——

We see that for the RM model $\mathcal{H} > 0.87$ is optimal. For the $(n,n,n+1)$ model optimal $\mathcal{H} \geq 0.87$ for all n and as n increases the optimal $\mathcal{H}$ approaches 1 and the model $(1,1,2)$ $(\mathcal{H} = 0.87)$ leads to smaller error than RM model with $\mathcal{H} = 0.87$.

In Table 4.12 we show the function β_{31} for the RM model $(\mathcal{H} = 0.87)$ and $(1,1,2)$ model with $\mathcal{H} = 1$ which are defined in the same way as in Table 4.4 for the (three-dimensional) plate model.

Table 4.12 The values of $\beta_{31}(x_1, x_2)$, $x_1 = 0.4,\ 0.5$ for various models (soft support)

x_2	$x_1 = 0.4$		$x_1 = 0.5$	
	RM	(1,1,2)	RM	(1,1,2)
0.49263	3.25	2.48	2.21	2.37
0.49500	3.24	3.47	2.23	2.41
0.49666	3.24	3.47	2.20	2.39
0.49878	3.23	3.47	2.04	2.24
0.49950	3.23	3.47	1.91	2.12
0.49989	3.24	3.47	1.83	2.03
0.49991	3.24	3.47	1.83	2.03
0.49994	3.23	3.47	1.83	2.03

It has been shown in [15] and [16] that when the boundary is smooth the strength of the boundary layer for the RM model is $\beta_{31} = \sqrt{12\mathcal{H}} = 3.23$. The detailed theoretical analyses of the boundary layer behavior of the (1,1,2) model is not available. In [17] was suggested that $\beta_{31}(0.5, x_2) \approx \sqrt{6\mathcal{H}} = 2.28$ for the RM model.

To the authors' knowledge there is no rigorous analysis of the boundary layer in the neighborhood of the corners of ω for RM or any other model.

We have seen that as $d \longrightarrow 0$ the difference between the soft and hard support disappears when measured in the energy norm. This is not true for the values influenced by the boundary layer. In Table 4.13 we show for the RM model with $\mathcal{H} = \frac{5}{6}$ the values $Q_{31}(0.5, 0.5)$ and $dQ_{31}(0.5, 0.5)$ for $d = 0.025$ and $d = 0.01$ for the soft support.

Table 4.13 The values of $Q_{31}(0.5, 0.5)$ as function of d

d	$Q_{31}(0.5, 0.5)$	$dQ_{31}(0.5,0.5)$
0.025	-2.68	-0.0671
0.01	-6.54	-0.0614

We see that dQ_{31} converges as $d \longrightarrow 0$ as expected (but not theoretically proven). We can expect (see [17]) that for the RM model $Q_{31}(0.5, 0.5)$ is proportional to $\sqrt{\mathcal{H}}$. In Table 4.14 we show that the expectation is correct.

Table 4.14 The dependence of $Q_{31}(0.5, 0.5)$ on $\mathcal{H}$ for the RM model.

$\mathcal{H}$	$Q_{31}(0.5, 0.5)$	$\mathcal{H}^{-1/2}Q_{31}(0.5, 0.5)$
1.0	-7.15	-7.15
0.91	-6.83	-7.16
0.87	-6.68	-7.16
5/6	-6.54	-7.16

4.5 The problem of the L-shaped domain.

In the previous Section we discussed the problem of the square plate. In this section we will briefly discuss the problem of the simply soft supported L-shaped plate. The domain ω is shown in Figure 4.7.

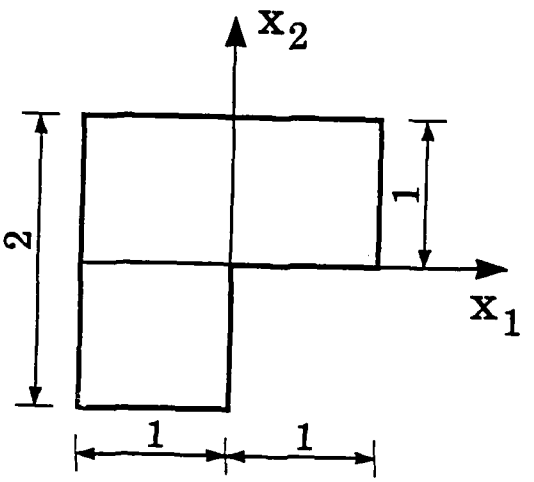

Figure 4.7 The L-shaped domain.

Once more we will consider the case $d = 0,01$ and $\nu = 0.3$. We will concentrate here on the behavior of the solution in the neighborhood of the origin where the solution is singular. We will present only the results of RM model for $\varkappa = 0.87$. Table 4.5 shows the theoretical strength of the singularities for the RM and K model for soft support ($\alpha = 270^{\circ}$).

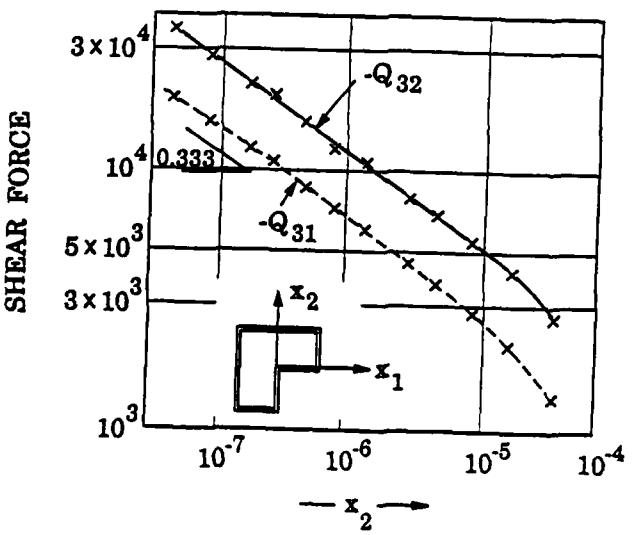

Figure 4.8 The shear force $Q_{31}(0, x_2)$, $Q_{32}(0, x_2)$ for the RM model.

Figure 4.8 shows in log log scale the shear forces on the line $x_1 = 0$ (as a function of x_2). In the figure we also show the expected theoretical slope (0.3333).

Figure 4.9 shows the values of the moments M_{22} and M_{12} as well as the theoretical slope. We see that the singularity is different for the moments and the shear forces.

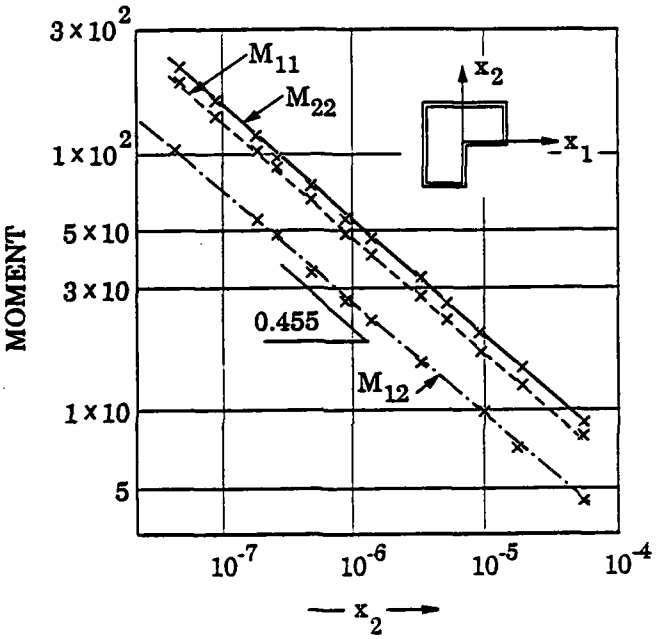

Figure 4.9 The moment $M_{22}(0, x_2)$, $M_{12}(0, x_2)$ for the RM model.

In Figures 4.10 and 4.11 we show the shear force Q_{32} and the moment M_{22} in a larger scale. We see that for $x_2 > 10^{-2}$ (i.e. of the thickness) the slope is 1.666 for Q_{32} and 0.666 for M_{22}. This behavior is related to the Kirchhoff singularity (also listed in Figure 4.5). We see typically that *inside* the domain, in the distance of order thickness the Kirchhoff model describes the character of the solution very well. This is typical behavior of the solution of every plate model as well as for the plate (three-dimensional) problem.

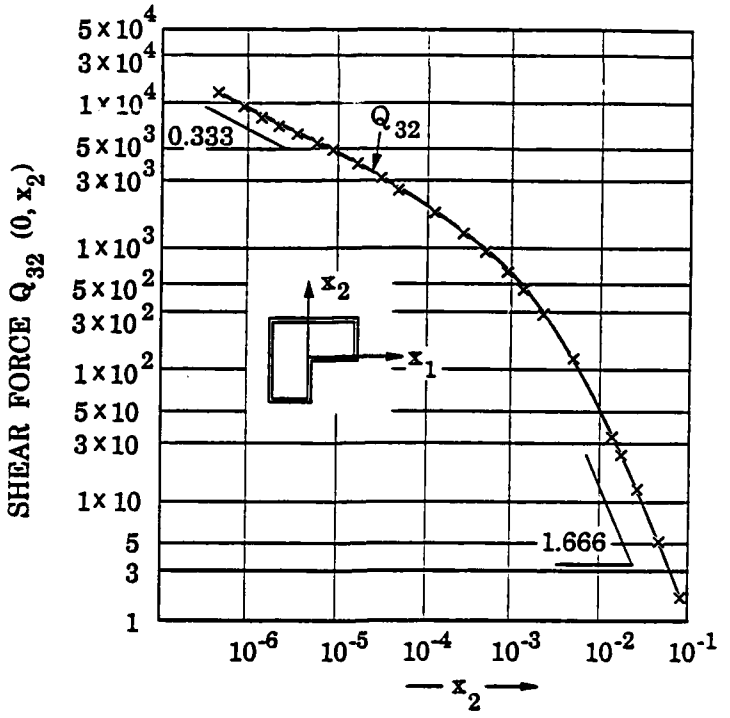

Figure 4.10 The shear force $Q_{32}(0, x_2)$.

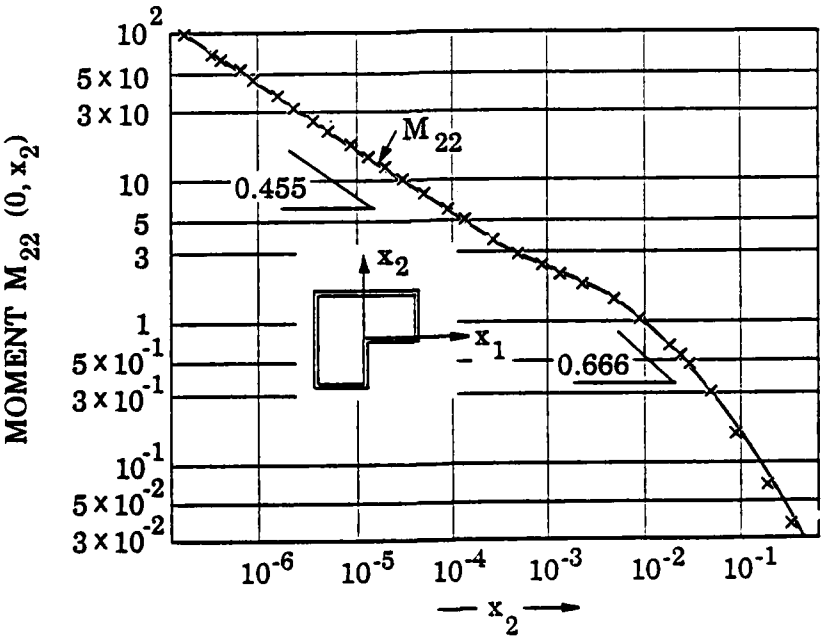

Figure 4.11 The moment $M_{22}(0, x_2)$

Figures 4.10 and 4.11 show the behavior *inside* ω. Figures 4.12 and 4.13 show the shear force $Q_{32}(x_1, 0)$ (the reaction) and the moment $M_{11}(x_1, 0)$.

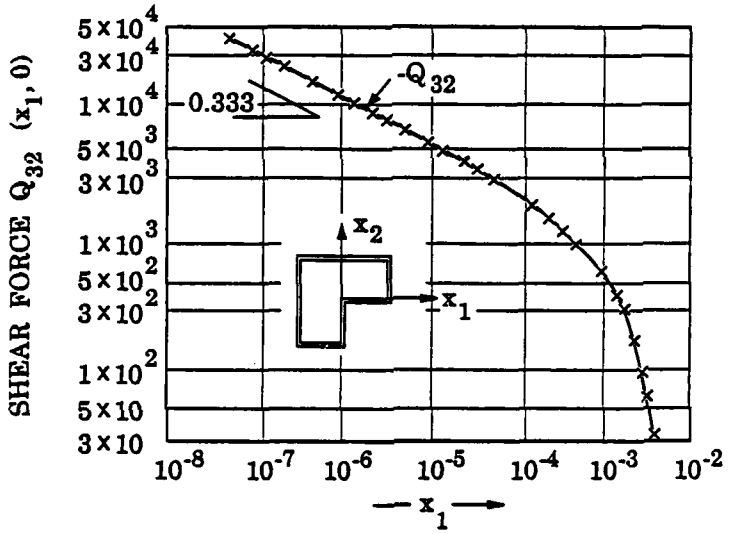

Figure 4.12 The shear force $Q_{32}(x_1, 0)$

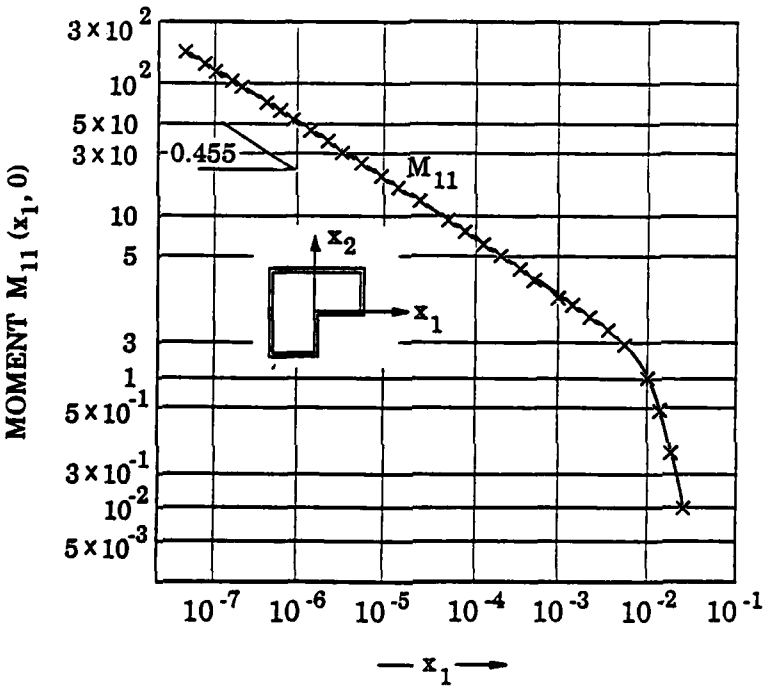

Figure 4.13 The moment $M_{11}(x_1, 0)$.

We see that the singularity in the close neighborhood of the vertex is the theoretical one as follows from Table 4.5. Nevertheless the Kirchhoff behavior is not visible because the line $x_2 = 0$ is on the boundary and the boundary layer is not captured by Kirchhoff model. The shear force $Q_{31}(x_1,0)$ does not show the singularity because of the influence of the boundary condition.

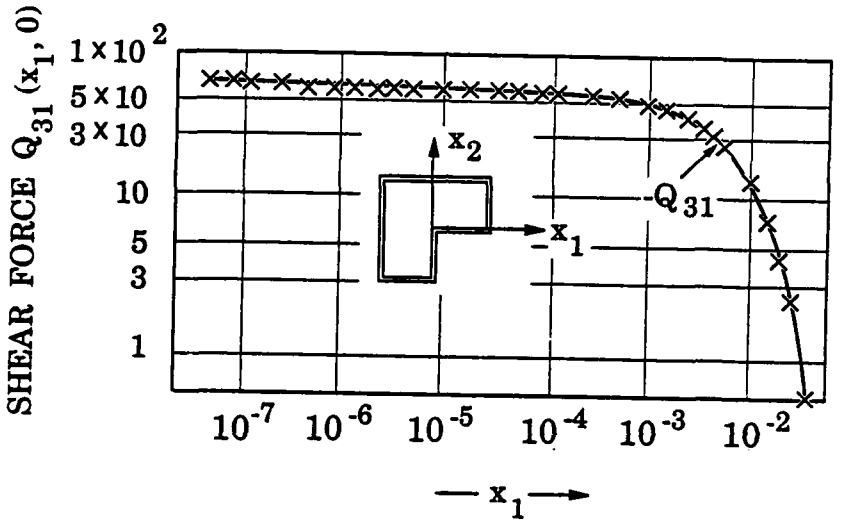

Figure 4.14 The shear force $Q_{31}(x_1,0)$.

We have shown the results and asymptotic behavior for the RM model only. They characterize well the behavior for any n-model as well as the solution of the three-dimensional solution.

We have seen that in the neighborhood of the vertex of ω we have exactly two kinds of singularities: one in the neighborhood which is smaller than the thickness and another one -- the Kirchhoff -- which is valid when the distance is of order of few thicknesses.

In Section 4.3 we introduced the (classical) Kirchhoff plate model with the solution $w = {}^{B}u_{B}^{k}$. The Kirchhoff model is not able to distinguish between the hard and soft simple support. Nevertheless the plate problem (three-dimensional as well as other plate models) converges (in the scaled energy norm) to the Kirchhoff solution as $d \longrightarrow 0$. See e.g. [2], [6] and Theorem 4.5.

The solution ω of the Kirchhoff model satisfies the biharmonic equation

$$D\Delta^2\omega = q \qquad (4.11)$$

$$D = \frac{d^3E}{12(1 - \nu^2)}$$

If ω is a polygon and simply support is considered the problem could be also formulated as follows: Find $w \in H^2(\omega)$ such that (4.11) holds and

$$w = \Delta w = 0 \qquad \text{on } \Gamma \text{ (except vertices of } \omega) \qquad (4.12)$$

This formulation is equivalent to the one based on the minimization of ${}^{B}G(u)$. Hence we can formulate the problem as the system

$$\Delta w = v$$

$$\Delta v = \frac{q}{D} \qquad (4.12)$$

$$w = v = 0 \qquad \text{on } \Gamma \text{ (except on the vertices of } \omega)$$

and $w \in H^2(\omega)$. The conditions that $w \in H^2(\omega)$ is essential. When ω is a *convex* polygon then ω can be found directly by (4.12). In this case $v \in H^2(\omega)$ and $w \in H^2(\omega)$. Nevertheless, when $\alpha > \pi$ then the solution of (4.12) yields $v \in H^1(\omega)$ and $w \in H^1(\omega)$ but $w \notin H^2(\omega)$ and so we have to

add (respectively subtract a singular function $\psi \in H^1(\omega)$) so that $w \in H^2(\omega)$. We have now

For $\alpha < \pi$, $\alpha \neq \frac{\pi}{2}$:

$$w = Cr^{\pi/\alpha}\psi(\theta) + \text{smoother terms}$$

For $\alpha > \pi$:

when $-\frac{\pi}{2} + 2 < \frac{2\pi}{\alpha}$, then

$$w = Cr^{-\pi/\alpha + 2}\psi(\theta) + \text{smoother terms}$$

when $\frac{2\pi}{\alpha} < -\frac{\pi}{\alpha} + 2$, then

$$w = Cr^{2\pi/\alpha}\psi(\theta) + \text{smoother terms}$$

when $\frac{2\pi}{\alpha} = -\frac{\pi}{\alpha} + 2$, then

$$w = r^{2\pi/\alpha}\left[C_1\psi_1(\theta) + C_2\psi_2(\theta)\right]$$

Here r,θ are polar coordinates with the origin in the vertex of the domain ω and $\psi(\theta)$ is a smooth function. The case $\alpha = \frac{\pi}{2}$ is an exceptional angle and then $w \in H^{5-\varepsilon}(\omega)$, $\varepsilon > 0$, arbitrary.

The moments M_{ij}, $i,j = 1,2$, and the shear forces Q_{3i}, $i = 1,2$, are given in the standard form

$$M_{11} = D\left[\frac{\partial^2 w}{\partial x_1^2} + \nu \frac{\partial^2 w}{\partial x_2^2} \right]$$

$$M_{22} = D\left[\nu \frac{\partial^2 w}{\partial x_1^2} + \frac{\partial^2 w}{\partial x_2^2} \right]$$

(4.13)
$$M_{12} = D(1-\nu)\left[\frac{\partial^2 w}{\partial x_1 \, \partial x_2} \right]$$

$$Q_{31} = D\left[\frac{\partial^3 w}{\partial x_1^3} + \frac{\partial^3 w}{\partial x_1 \partial x_2^2} \right]$$

$$Q_{32} = D\left[\frac{\partial^3 w}{\partial x_1^2 \partial x_2} + \frac{\partial^3 w}{\partial x_2^3} \right]$$

and hence

$$M_{ij} = Cr^{\lambda_1 - 1}\psi_{i,j}(\theta) + \text{smoother terms}$$

$$Q_{3j} = Cr^{\lambda_2 - 1}\psi_j(\theta) + \text{smoother terms}$$

As before the coefficients λ_1 and λ_2 for the Kirchhoff model are given in Table 4.5.

As was previously mentioned, the Kirchhoff model cannot distinguish between hard and soft support. We show now that the Kirchhoff model should be understood as *an approximation of the hard support* although sometimes it is used for the soft support also (see below).

In Table 4.15 we show the error of the Kirchhoff model when compared with the solutions of the (three-dimensional) plate problem of the square uniformly loaded plate ($\nu = 0.3$, $d = 0.01$) for $d = 0.1$ and $d = 0.01$.

Table 4.15 Comparison of the energy of the Kirchhoff model.

d	$\left[\frac{\lvert\varepsilon^B(w) - \varepsilon^A(u^H)\rvert}{\varepsilon^A(u^S)}\right]^{1/2}$	$\left[\frac{\lvert\varepsilon^B(w) - \varepsilon^A(u^S)\rvert}{\varepsilon^A(u^S)}\right]^{1/2}$
0.1	20.31%	39.56%
0.01	2.03%	11.87%

In Table 4.16 we show for $d = 0.01$ some comparison of data from the Kirchhoff model and the three-dimensional solution.

Table 4.16 Comparison of shear forces and moments of the Kirchhoff and three-dimensional model ($d = 0.01$).

	$Q_{31}(0.4,\ 0.5)$	$Q_{31}(0.5\text{-}0,\ 0.5)$	$M_{12}(0.5\text{-}0,\ 0.5)$
hard support	0.	0.	0.0325
soft support	-9.72	-6.79	0.
Kirchhoff	0.	0.	0.0325

In the table we denoted

$$Q_{3,1}(0.5\text{-}0,\ 0.5) = \lim_{\substack{x_1<0.5 \\ x_1 \to 0.5}} Q(x_1,\ 0.5)$$

Kirchhoff model also reproduces the paradox of the hard simple support i.e. we have $w_m \longrightarrow w_c$ as $m \longrightarrow \infty$ (see Theorem 4.2) and [6], [13] and [14].

Often in the Kirchhoff theory the reaction e.g. $V_2 = Q_{32}$ (for $x_2 = 0.5$) is computed from the formula

$$V_2 = \left[Q_{32} - \frac{\partial M_{12}}{\partial x_1}\right] \tag{4.14}$$

see e.g. [18]. This derivation tries to simulate the reaction for the *soft* simple support when using essentially the data from the hard support. The main idea of the standard derivation of (4.14) is following: The virtual work by the Kirchhoff theory can be written in the form

$$(4.15) \qquad B(w,v) = \int_W qvdx - \oint Q_n v dt + \oint \left[M_n \frac{\partial v}{\partial n} + M_{nt} \frac{\partial v}{\partial t} \right] dt$$

Here we denoted by M_n the normal moment (for the simple support $M_n = 0$) and M_{nt} is the twist moment. By integration by parts in (4.15) we get

$$(4.16) \qquad B(w,v) = \int_W qvdx - \oint \left[Q_n + \frac{\partial M_{nt}}{\partial t} \right] v dt + \oint_\Gamma M_n \frac{\partial v}{\partial n} dt$$

Here $\frac{\partial M_{nt}}{dt}$ is (generalized) derivative with respect to the tangent. We remark that M_{nt} is discontinuous by (in the case of the square domain) piecewise smooth and hence $\frac{\partial M_{nt}}{dt}$ is a Dirac function (concentrated force) in the vertex with the value of the "jump" in the moment. In the general case, for example when $\alpha \geq \frac{\pi}{2}$, then the "jump" is infinite and so it is not completely plausible to make a reasonable physical interpretation. The idea in deriving (4.16) is to remove the virtual work by the twist moment but still keep the same value of the total virtual work. In the case of the square plate ($\alpha = 90^\circ$) the concentrated force computed through the twist moment is relatively successful. We get here $\mathcal{R} = 0.0325 = M_{12}(0.5, 0.5)$ computed with the exact value $\mathcal{R}$ defined in Section 4.2 ($\mathcal{R} = 0.0290$) and the difference is about 10%.

4.7 Summary and conclusions.

The simple support is an idealization which does not necessarily

describe the reality well. There are many possible formulations. We mentioned only two possibilities, the hard and soft simple support. There are others. For example we mention the notion of the supersoft support which is defined so that $\mathcal{H}(\Omega) = \{u \mid \int_{-d/2}^{d/2} u_3(x_1,x_2,x_3)dx_3 = 0, \quad (x_1,x_2) \in \Gamma\}$ instead $u_3(x_1,x_2,x_3) = 0$ as was assumed. This will influence the solution by still various basic features discussed earlier for the soft support will occur.

In the literature sometimes another formulation of the soft support is used. Here $\mathcal{H}(\Omega) = \{u \mid u(x_1,x_2,0) = 0, \quad (x_1,x_2) \in \Gamma\}$. Nevertheless this formulation has no sense because for the 3-dimensional formulation the quadratic functional $G(u)$ will be not bounded from below and the solution does not exist. (The essential reason is that under a concentrated load (reaction) the displacement is infinite.)

Comparing the results we mentioned earlier we see:

(1) The Kirchhoff model gives completely unreliable results in the neighborhood of the boundary (of size of the plate thickness) although it gives acceptable results inside the domain. It approximates much better the hard support than the soft support. In the close neighborhood of the vertices the Kirchhoff model leads to the singularities which are very different when compared with the exact solution of the 3-dimensional problem.

(2) There is a significant difference between the solution for the hard and soft simple support. This difference is limited to the neighborhood of the boundary. The size of the neighborhood depends on the smoothness of the boundary. The soft support does not have certain paradoxical properties which the hard one has.

(3) The RM model performs well. The shear factor $\varkappa$ has a positive influence on the quality of the solution. Nevertheless, the optimal value depends on the concrete setting and aims of computation. In the given case the value $\varkappa = 0.87$ is close to optimal.

(4) The singularity of the (1,1,2) model is the same as of the three-dimensional solution. The RM model leads to a slightly different singularity.

(5) The singular behavior of the RM model and the n-model is well described by the theory which is valid in the area of approximately $\frac{1}{2}$ + 1 thickness. In the areas of larger distance the solution has singular behavior well described by the Kirchhoff model.

(6) The RM model ($\varkappa = 0.87$) performs better than the model (1,1,2) with $\varkappa = 1$ (not with $\varkappa = 0.87$) but the model (3,3,4) with $\varkappa = 1$ outperforms RM.

(7) The negative reaction of the solution of the three-dimensional solution, RM model, and n-model differs approximately 10% from the Kirchhoff negative concentrated reaction.

5. The plate problem for various boundary conditions.

In Section 4 we addressed in detail the problem of the square simply supported plate. In this section we will briefly analyze the essentials when other boundary conditions are imposed especially with respect to the differences to the case discussed earlier.

5.1 The square clamped plate.

Let us consider the square plate with all build in boundary conditions. Here $\mathcal{H}(\Omega) = \{u \mid u = 0 \text{ on } S\}$. As before, we can similarly define RM model, n-model, and Kirchhoff model.

Analogous to our previous analysis, we use the matrix B and parameter $\mathcal{H}$ for the RM model. Then as $d \longrightarrow 0$ the difference (measured in the scaled energy norm) converges to zero. Hence the problem has quite analogous properties as before.

For the numerical analysis we still consider as before the unit square plate, $d = \frac{1}{100}$, $\nu = 0.3$ and for the RM model we will use $\mathcal{H} = 0.87$, for the n-model we will use $\mathcal{H} = 1$. In Tables 5.1 and 5.2 we report the moment $M_{11}(x_1, x_2)$ and $M_{22}(x_1, x_2)$ for $x_1 = 0$, $x_2 = 0.2777$ respectively. The moment $M_{11}(x_1, 0)$ is essentially identical ($\varepsilon < 0.1\%$) for all three models considered. Hence no error is present. On the other hand, the error in $M_{22}(x_1, 0)$ for the RM model is large (30%), while for the (1,1,2) model it is acceptable. Here we see a significant difference in comparison to the simple support. Let us mention that the Kirchhoff plate model yields $M_{11}(0, 0.5) = 0.0513$, $M_{22}(-0, 0.5) = 0.0153$, i.e. the identical results as the RM model.

Moment M_{22} has a boundary layer which *is not* captured by the RM model. As in Section 4.2 (see Table 4.4) we define $\beta_{22}^{(n)}(x_1, x_2)$ so that

$$\exp\left[-\beta_{22}^{(n)}(x_1, x_2)\,\frac{(0.5 - x_1)}{d}\right] = \frac{|M_{22}^{RM}(x_1,\ x_2) - M_{22}^{(n)}(x_1,\ x_2)|}{|M_{22}^{RM}(0.5,\ x_2) - M_{22}^{(n)}(0.5,\ x_2)|}$$

where the function $\beta_{22}(x_1, x_2)$ characterizes the boundary layer. We use in the above formula $M_{22}^{RM}(x_1, x_2)$ as natural smooth extension of $M_{22}^{n}(x_1, x_2)$ from the inside where $M_{22}^{n} = M_{22}^{RM}$. In Table 5.3 we show a few values of $\beta_{22}^{(1,1,2)}$ and $\beta_{22}^{3\ dim}$.

Table 5.1 The moments $M_{11}(x_1,0)$, $M_{22}(x_1,0)$ for different plate models.

	$M_{11}(x_1,0)$			$M_{22}(x_1,0)$				
x_1	3 dim	RM	(1,1,2)	3 dim	RM	ε_{RM}%	(1,1,2)	ε_{112}%
0.	-0.0229	-0.0229	-0.0229	-0.0229	-0.0229	0.	-0.0229	0.
0.2000	-0.0157	-0.0157	-0.0157	-0.0163	-0.0163	0.	-0.0163	0.
0.4000	0.0164	0.0163	0.0164	0.0026	0.0027	0.	0.0026	0.
0.4900	0.0470	0.0470	0.0470	0.0141	0.0141	0.	0.0141	0.
0.4930	0.0483	0.0483	0.0483	0.0145	0.0144	0.	0.0144	0.
0.4990	0.0509	0.0509	0.0509	0.0168	0.0152	9.2	0.0170	1.4
0.4995	0.0510	0.0510	0.0510	0.0176	0.0153	12.3	0.0179	2.1
0.4999	0.0512	0.0512	0.0512	0.0207	0.0153	25.3	0.0212	2.8
0.5000	0.0513	0.0513	0.0513	0.0220	0.0153	30.0	0.0220	0.

Table 5.2 The moments $M_{11}(x_1,0.2777)$, $M_{22}(x_1,0.2777)$ for different plate models.

	$M_{11}(x_1,0.2777)$			$M_{22}(x_1,0.2777)$				
x_1	3 dim	RM	(1,1,2)	3 dim	RM	ε_{RM}%	(1,1,2)	ε_{112}%
0.	-0.0102	-0.0102	-0.0102	-0.0075	-0.0075	0.	-0.0075	0.
0.2000	-0.0075	-0.0075	-0.0075	-0.0058	-0.0058	0.	-0.0058	0.
0.4000	0.0083	0.0083	0.0083	0.0015	0.0015	0.	0.0015	0.
0.4900	0.0256	0.0256	0.0256	0.0077	0.0077	0.	0.0077	0.
0.4930	0.0263	0.0263	0.0263	0.0079	0.0079	0.	0.0079	0.
0.4990	0.0279	0.0279	0.0279	0.0092	0.0084	9.2	0.0093	1.4
0.4995	0.0280	0.0280	0.0280	0.0096	0.0084	9.0	0.0098	2.0
0.4999	0.0281	0.0281	0.0281	0.0113	0.0084	25.3	0.0116	2.7
0.5000	0.0281	0.0281	0.0281	0.0121	0.0084	30.1	0.0121	0.1

Table 5.3 The coefficient $\beta_{22}(x_1,0)$ for the clamped plates.

x_1	3 dim $\beta_{22}(x_1,0)$	(1,1,2) $\beta_{22}(x_1,0)$
0.4990	15.43	13.86
0.4996	18.17	13.41
0.4999	23.85	13.32
0.49993	24.13	13.31
0.49999	24.78	13.29

We see that the RM model does not have essentially any boundary layer for the clamped boundary condition. This follows from [15], [16]. On the other hand the model (1,1,2) and the plate problem shows a strong boundary layer. The theoretical strength of the solution of (1,1,2) model is $\sqrt{\frac{120}{1-\nu}} = 13.1$ (see [19]) which is very close to the values shown in Table 5.3. The exact solution shows still stronger boundary layer.

5.2 The plate with two opposite sides clamped and two free.

In this section we will consider the case when the type of the boundary condition is changing in the vertex. We will consider the unit square domain with the sides $x_2 = \pm 0.5$ to be clamped and $x_1 = \pm 0.5$ to be free. The boundary condition in the vertex $A = (0.5, 0.5)$ changes the type from one side to the other. Once more as $d \longrightarrow 0$ the solution of the plate problem (three-dimensional) as well as the n-model solution converges in (scaled) energy norm to the Kirchhoff solution. See for example arguments in [2], [6]. In the neighborhood of the vertex A the solution has singular

behavior. Denoting by r the distance from the vertex A we have

$$M_{ij} = C_1 r^{\lambda_1 - 1} \psi_{ij}(\theta) + \text{smoother terms}$$

$$Q_{3j} = C_2 r^{\lambda_2 - 1} \psi_j(\theta) + \text{smoother terms}$$

Where λ_1 and λ_2 are different for different models. Their values for our case are given in Table 5.4.

The value $\lambda_2 = 1$ for the RM and (1,1,2) model means that for this singularity the angle is exceptional and the shear force Q_{3j} is bounded in the neighborhood of A.

Table 5.4 The singularity coefficients λ_1, λ_2 for various models.

	RM	(1,1,2) 3 dim	K
λ_1	0.7583	0.7112	1.0687 + i 0.4386
λ_2	1.	1.	0.687 + i 0.4386

Let us now consider the case as in the previous section, namely $d = 0.01$, $\nu = 0.3$. Figure 5.1 shows moment M_{22} on the line $x_1 = x_2$ of the (three-dimensional) solution of the plate problem as a function of the distance r from the point A.

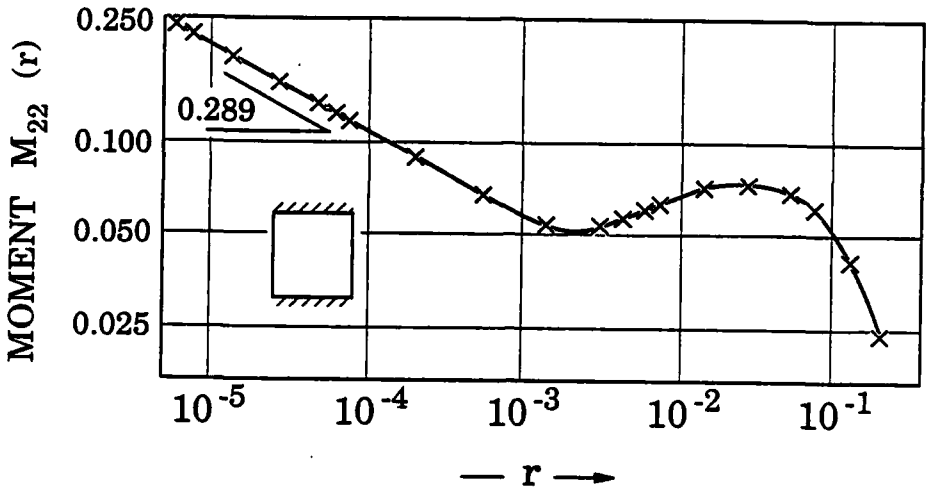

Figure 5.1 The moment $M_{22}(r)$ on the line $x_1 = x_2$ for the three-dimensional solution.

In Figure 5.1 we also show the theoretical singularity -0.289 as follows from Table 5.4. For $r > 10^{-2}$ the moment shows the character of the Kirchhoff singularity where the singularity coefficient is complex.

In Figure 5.2 we show in more detail in log log scale the moment for the RM model and three-dimensional solution. We clearly see different growth as follows from Table 5.4.

Figure 5.3 shows the behavior of the moments M_{11}, and M_{22} and shear force Q_{32} from the RM model. We clearly see the growth in accordance with Table 5.4.

As we have seen in Figure 5.1, the moment M_{22} shows oscillations. To understand this oscillation better we show in Figure 5.4, the moment M_{22} of the RM model as a function of Lg r. In addition we show the function $C\cos(0.4386 \lg \frac{r}{r_0})$ as approximations by the function having the Kirchhoff type singularity. We see very good agreement.

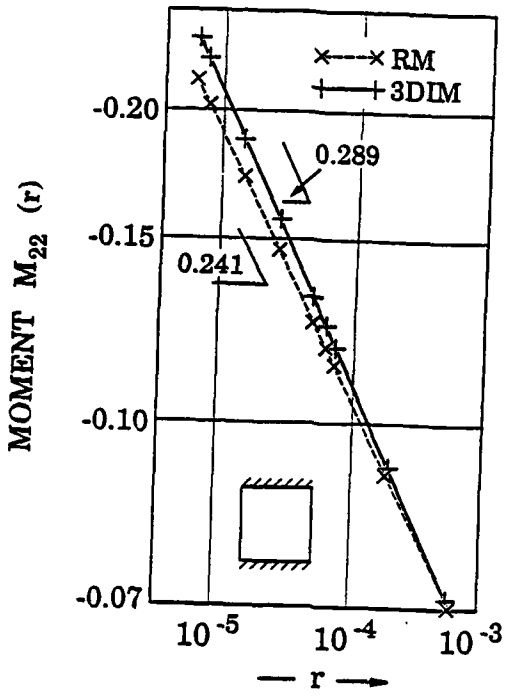

Figure 5.2 The moment $M_{22}(r)$ for the RM model and three-dimensional solution.

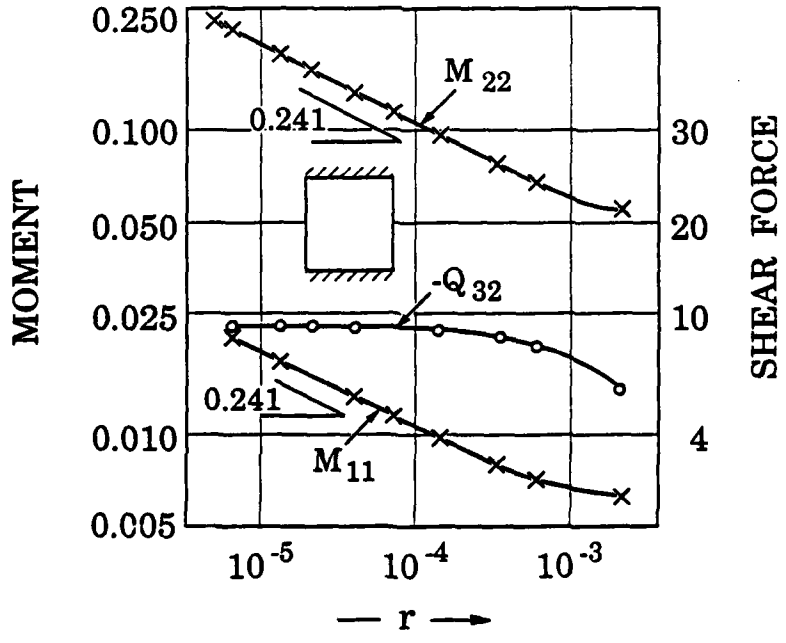

Figure 5.3 The moments M_{11}, M_{22} and the shear force Q_{32} of the RM model.

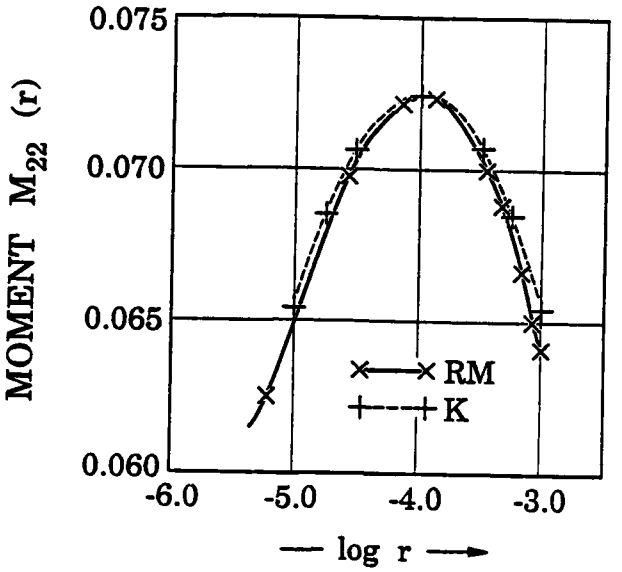

Figure 5.4 The moment M_{22} of RM solution and its approximation by Kirchhoff type singularity.

Table 5.5 The moment M_{22} on $x_1 = x_2$ for various models.

x_1	3 dim	RM $\mathcal{H}$ = 0.91	ε%	RM $\mathcal{H}$ = 0.91	ε%	RM $\mathcal{H}$ = 5/6	ε%	(1,1,2)	ε%
0.	-0.0407	-0.0407	0.	-0.0407	0.	-0.0407	0.	-0.0407	0.
0.135	-0.0317	-0.0317	0.	-0.0317	0.	-0.0317	0.	-0.0317	0.
0.27	-0.0048	-0.0048	0.	-0.0048	0.	-0.0048	0.	-0.0048	0.
0.36	0.0239	0.0238	0.	0.0238	0.	0.0238	0.	0.0238	0.
0.45	0.0612	0.0612	0.	0.0612	0.	0.0612	0.	0.0612	0.
0.4635	0.0670	0.0670	0.	0.0670	0.	0.0670	0.	0.0670	0.
0.4815	0.0722	0.0722	0.	0.0722	0.	0.0722	0.	0.0722	0.
0.4953	0.0624	0.0626	0.2	0.0627	0.4	0.0627	0.4	0.0621	0.5
0.4968	0.0575	0.0576	0.1	0.0578	0.5	0.0579	0.7	0.0567	1.3
0.4995	0.0630	0.0624	0.9	0.0632	0.4	0.0640	1.6	0.0605	4.0
0.49995	0.1173	0.1125	4.0	0.1140	2.7	0.1154	1.6	0.1143	2.5
0.499995	0.2252	0.1989	11.7	0.2014	10.5	0.2038	9.5	0.2212	1.7

In Table 5.5 we show some values of the moment M_{22} for various models. We see that for $x \approx 0.5$ the moments of the model (1,1,2) are better than for the RM model. It relates directly to the different singular behavior of the solution from the various models, as follows from Table 5.4.

5.3 Summary and conclusions.

Let us mention some conclusions which follow from our analysis:

1) The boundary layer behavior of the RM model as described in [15] [16] is very weak for the clamped boundary condition. Nevertheless the strong boundary layer is present for the three-dimensional formulation as well as (1,1,2) model. The RM model leads to a very large error here when compared with the exact solution of the three-dimensional problem. In contrast the model (1,1,2) gives very acceptable results.

2) Changing the type of boundary conditions in the vertex usually leads to different singular behavior of the solution of the RM model and three-dimensional solution. The model (1,1,2) has the same strength of the singularity as the three-dimensional solution. Hence the RM model yields a large error in a very small neighborhood of the vertex. The structure of the solution is further complicated by the different strengths of boundary layer on the sides with different boundary conditions.

6. Additional remarks and conclusions.

The solution of the plate problem is very sensitive to boundary conditions in the neighborhood of the boundary. Different models lead in

general to very different boundary layer behavior and singularities in the neighborhood of the vertices of the domain. We discussed only the behavior of the moments and shear forces, i.e. of the resultants, the detailed solution (stresses) has still more complicated structure (see e.g., [20]).

The singular and boundary layer behavior of course strongly influences the accuracy of the numerical solution and requires very careful mesh design.

If the plate is relatively thin, say $\frac{1}{100}$ of the diameter, the sensitivity of the data inside of ω is much smaller than in the boundary layer. Nevertheless it still can be large.

The design of the model has to be directly related to the aims of computations. For example the Kirchhoff model typically could lead to results which are very far from the exact three-dimensional solution if the data at the boundary are of interest. (These data are reported in any book about plate theory.) Inside of the domain the Kirchhoff data usually are relative reliable but it depends on the type of boundary conditions and the structure of the plate domain.

Reissner-Mindlin model performs well and captures well the boundary layer behavior for some boundary conditions; nevertheless it fails completely for some others such as clamped boundary conditions and could yield results with error of 30%. The (1,1,2) model especially with a shear factor is much more relevant and gives reliable data also when RM fails as in the case of the clamped boundary condition. This model also has the same singular behavior as the solution of the (three-dimensional) plate model, while the RM often has different singularity. The singularity of the solution of the Kirchhoff model is *completely different* when compared with the singular behavior of the solution of three-dimensional problem.

The selection of the plate model has to be related to the aims of

computation and the best way is to select it in an adaptive feature from a family of hierarchical models; in different plate areas. In addition a-posteriori error of the solution when compared with the exact three-dimensional solution is desirable and can be made by comparing the results from different hierarchically ordered models.

Finally we mention that the boundary layer influences the accuracy of the finite element solution and has to be dealt with. (For example by an adaptive solver. Furthermore, the finite element solution of the n-model leads to the locking effects which are dealt with in various ways. In [21] we have shown that the p-version of FEM for $p \geq 4$ does not show practically the locking effects.

References

[1] Noor, A.K., Scott Burton, W. [1989]: Assessment of shear deformation theories for multilayered composite plates, Appl. Mech. Rev. 42, 1-12.

[2] Morgenstern, D. [1959]: Herleidung der Plattentheorie aus der dreidimensionalen Elastizitätstheorie, Arch. Rational Mech. Anal. 4, 145-152.

[3] Destuynder, P. [1986]: *Une Théorie Asymptotigne des Plagues Minces en Elasticité Linéaire*, Masson, Paris.

[4] Ciarlet, P.G. [1990]: *Plates and junctions in elastic multi-structures, An asymptotic analysis*, Masson, Paris, Springer, Berlin.

[5] Schwab, Ch. [1989]: The dimensional reduction method, Ph.D. Thesis, University of Maryland, College Park, Maryland, 20742, U.S.A.

[6] Babuška, I., Pitkäranta, J. [1990]: The plate paradox for hard and soft simple support, SIAM J. Math. Anal. 21, 551-576.

[7] Dauge, M. [1988]: *Elliptic Boundary Value Problems on Corner Domains*, Lecture Notes in Math 1341, Springer, New York, 1988.

[8] Petersdorff, T. [1989]: Randwertprobleme der Elastizitätstheorie für Polyeder Singularitäten und Approximation mit Randenelement Methoden, Ph.D. Thesis, T.H. Darmstadt, Federal Republic Germany.

[9] Li, L., Babuška, I. [1991]: On the corner singularities of the solution of various plate bending models, Tech. Note, Institute for Physical Science and Technology, University of Maryland, College Park, Maryland, 20742.

[10] Reissner, E. [1947]: On bending of Elastic Plates, Quart. of Appl. Math. 5, 55-69.

[11] Mindlin, R.D. [1951]: Influence of Rotatory Inertia and Shear Flexural Motions of Isotropic Elastic Plates, Journ. Appl. Mech. 18, 31-38.

[12] Cowper, G.R. [1966]: The Shear Coefficient in Timoshenko's Beam Theory, Journ. Appl. Mech. 33, 331-340.

[13] Babuška, I. [1961]: The stability of the domain of definition with respect to basic problems of the theory of partial differential equations especially with respect to the theory of elasticity I, II, Czechosl. Math. J., 76-105, 1065-203, (in Russian).

[14] Maz'ja, V.G., Nazarov, S.A. [1984]: About the Sapondzhyn-Babuška Paradox in the Plate Theory, Dokl. Akad. Nauk. Arm. Rep. 78, 127-130 (in Russian).

[15] Arnold, D.N., Falk, R.S. [1989]: Edge Effects in the Reissner-Mindlin Plate Theory, in *Analytical and Computational Models of Shells*, ed. A.K. Noor, T. Belitsko, S. Simo, ASME, 71-90.

[16] Arnold, D.I., Falk, R.S. [1990]: The Boundary Layer for Reissner-Mindlin Plate Model: Soft Simply Supported, Soft-Clamped and Free Plates, SIAM J. Math. Anal. 21, 281-312.

[17] Häggblad, B., Bathe, K.J. [1991]: Specifications of Boundary Conditions for Reissner-Mindlin Theory Based on Plate Bending Finite Elements, Int. J. for Num. Meth. Engng.

[18] Timoshenko, S., Woinowski-Krieger, S. [1959]: *Theory of Plates and Shells*, Sec. ed., McGraw-Hill.

[19] Li, L. Babuška, I. [1990]: On the Reissner-Mindlin plate and the (1,1,2) model for the clamped-in plane problem, Tech. Note BN 1117, Institute for Physical Science and Technology, University of Maryland, College Park, Maryland, 20742.

[20] Babuška, I. [1990]: The problem of modeling the elastomechanics in engineering, Comp. Meth. in Appl. Mech. Engrg. 82, 155-182.

[21] Babuška, I., Li, L. [1990]: The h-p Version of the Finite Element Method in the Plate Modeling Problem, Tech. Note BN 1115, Institute for Physical Science and Technology, University of Maryland, College Park, Maryland, 20742.

The Laboratory for Numerical Analysis is an integral part of the Institute for Physical Science and Technology of the University of Maryland, under the general administration of the Director, Institute for Physical Science and Technology. It has the following goals:

- To conduct research in the mathematical theory and computational implementation of numerical analysis and related topics, with emphasis on the numerical treatment of linear and nonlinear differential equations and problems in linear and nonlinear algebra.

- To help bridge gaps between computational directions in engineering, physics, etc., and those in the mathematical community.

- To provide a limited consulting service in all areas of numerical mathematics to the University as a whole, and also to government agencies and industries in the State of Maryland and the Washington Metropolitan area.

- To assist with the education of numerical analysts, especially at the postdoctoral level, in conjunction with the Interdisciplinary Applied Mathematics Program and the programs of the Mathematics and Computer Science Departments. This includes active collaboration with government agencies such as the National Institute of Standards and Technology.

- To be an international center of study and research for foreign students in numerical mathematics who are supported by foreign governments or exchange agencies (Fulbright, etc.).

Further information may be obtained from **Professor I. Babuska**, Chairman, Laboratory for Numerical Analysis, Institute for Physical Science and Technology, University of Maryland, College Park, Maryland 20742.